TÜRKİYE CUMHURİYETİ
ADANA ALPARSLAN TÜRKEŞ SCIENCE AND TECHNOLOGY UNIVERSITY

GRADUATE SCHOOL
BIOENGINEERING DEPARTMENT

PREPARATION OF STIGMASTEROL IMPRINTED SOLID PHASE EXTRACTION POLYMERS FOR SEPERATION OF STIGMASTEROL FROM PLANT EXTRACTS

BÜRGE ÇELEBİ

M.Sc.

ADANA 2023

TÜRKİYE CUMHURİYETİ
ADANA ALPARSLAN TÜRKEŞ SCIENCE AND TECHNOLOGY UNIVERSITY

GRADUATE SCHOOL
BIOENGINEERING DEPARTMENT

PREPARATION OF STIGMASTEROL IMPRINTED SOLID PHASE EXTRACTION POLYMERS FOR SEPERATION OF STIGMASTEROL FROM PLANT EXTRACTS

BÜRGE ÇELEBİ

M.Sc.

THESIS ADVISOR
PROF. DR. GÖZDE BAYDEMİR PEŞİNT

ADANA, 2023

DECLARATION OF CONFORMITY

In this thesis study, which was prepared following the thesis writing rules of Adana Alparslan Türkeş Science and Technology University Institute of Graduate School, I declare that I provide all the information, documents, evaluations and results in accordance with scientific ethics and moral codes without resorting to any means or assistance that would be contrary to scientific ethics and traditions. I also declare that I refer to all of the articles I used in this study with appropriate references and accept all moral and legal consequences if a situation is found contrary to my statement regarding my work.

30/12/2022

[Signature]

Bürge ÇELEBİ

ÖZET

STİGMASTEROLÜN BİTKİ EKSTRAKTLARINDAN AYRIŞTIRILMASI İÇİN STİGMASTEROL BASKILANMIŞ KATI FAZ EKSTRAKSİYON POLİMERLERİNİN HAZIRLANMASI

Bürge ÇELEBİ
Yüksek Lisans, Biyomühendislik Anabilim Dalı
Danışman: Prof. Dr. Gözde BAYDEMİR PEŞİNT

Ocak 2023, 55 sayfa

Stigmasterol (Stg) bitkilerde serbest alkoller şeklinde ya da onların çökeltileri halinde, özellikle bitkisel yağlarda doğal halde bulunan fitosterol ailesinin bir üyesidir. Fitosterollerin insan sağlığına etkisi üzerine yapılan araştırmalarda bireylerin fitosterol alımı ile düşük yoğunluklu lipoprotein yani kolesterol düşürücü etkilerinin olduğu bildirilmiştir. Bulunan birçok değerli bileşende potansiyel olanlardan biri olan Stg, bugüne kadar birçok bitkiden izole edilmiş ve birçok farmakolojik ve biyolojik aktivite için değerlendirilmiştir. Ayrıca anti-inflamatuar, anti-osteoartrit, anti-aterojenik, antioksidan ve plazma kolesterol seviyelerini düşürme gibi sağlık üzerine olumlu etkileri ve anti kanser gibi koruyucu etkileri de bilinmektedir. Bu çalışmada, bitki örneğinden doğrudan Stg tayini için Stg baskılı katı faz ekstraksiyon polimerlerinin hazırlanması amaçlanmıştır. MAA, VBA, DVB-80 ve AIBN kullanılarak moleküler baskılanmış polimer çözeltisi hazırlanmıştır, sentezlenen polimerler daha sonra taramalı elektron mikroskobu (SEM), şişme testleri ve fourier transform infrared spektroskopisi (FTIR) ile karakterize edilmiştir. Stg-MIP polimerlerinin stigmasterol molekülü için seçiciliği, kolesterol ve ergosterol yarışmacı moleküllerine karşı incelenmiştir. Bu çalışmada Stg-MIP polimerlerinin tekrar kullanılabilirlikleri de incelenmiştir. Stg-MIP polimerleri, aynı adsorbent kullanılmak koşuluyla tekrarlanabilirlik deneyleri gerçekleştirilmiş ve adsorpsiyon kapasitesinde ciddi bir düşüş gözlemlenmemiştir.

Anahtar Kelimeler: Stigmasterol, moleküler baskılama teknolojisi, eş boyutlu küreler

ABSTRACT

PREPARATION OF STIGMASTEROL IMPRINTED SOLID PHASE EXTRACTION POLYMERS FOR SEPERATION OF STIGMASTEROL FROM PLANT EXTRACTS

Bürge ÇELEBİ

M.Sc., Department of Bioengineering

Supervisor: Prof. Dr. Gözde BAYDEMİR PEŞİNT

January 2023, 55 pages

Stigmasterol (Stg) is a member of the phytosterol family, which is found naturally in plants in the form of free alcohols or in their sediments, especially vegetable oils. In studies on the effects of phytosterols on human health, it has been reported that individuals have low-density lipoprotein (cholesterol) lowering effects with phytosterol intake. Stg, one of the many valuable ingredients found, has been isolated from many plants to isolate and evaluated for many pharmacological and biological activities. It is also known to have positive effects on health such as anti-inflammatory, anti-osteoarthritis, anti-atherogenic, antioxidant and lowering plasma cholesterol levels, and protective effects such as anti-cancer. In this study, it was aimed to prepare Stg-imprinted solid phase extraction polymers for direct determination of Stg from plant extract. Molecular imprinted polymer solution was prepared using MAA, VBA, DVB-80 and AIBN, the synthesized polymers were then characterized by scanning electron microscopy (SEM), swelling tests and fourier transform infrared spectroscopy (FTIR). The selectivity of Stg-MIP polymers for the Stg has been studied against the competitor molecules of cholesterol and ergosterol. In this study, the reusability of Stg-MIP polymers was also examined. Stg-MIP polymers were used more than once for reproducibility experiments with the same adsorbent condition, and results showed a minimal loss in adsorption capacity.

Keywords: Stigmasterol, molecular imprinting technology, monosize spheres

ACKNOWLEDGEMENTS

I would like to sincerely thank my dear supervisor, Prof. Dr. Gözde BAYDEMİR PEŞİNT, who guided me with her experience and understanding during my master's education and my thesis.

I sincerely thank my dear teammates; Burcu EREN YÜNGEVİŞ, Kardelen CEMEK, Okan ZENGER for helping and supporting me during my thesis.

I would also like to give special thanks to my love, husband, Koray ÇELEBİ and my family as a whole for their valuable support and understanding when undertaking my studies.

This thesis was financially supported by ATU BAP Coordination Unit with project number of 21303023.

TABLE OF CONTENTS

LIST OF FIGURES

LIST OF TABLES

LIST OF ABBREVIATIONS

MIP	: Molecularly Imprinted Polymer
UV	: Ultraviolet
Stg	: Stigmasterol
VBA	: 4-vinly benzylalcohol
MAA	: Methacrylic acid
DVB-80	: Divinylbenzene-80
AIBN	: 2,2-azo-bis-isobutyronitrile
DVB	: Divinylbenzene
ATPase	: Adenosine triphosphatase
H	: Hidrogen
HPLC	: High-performance liquid chromatography
FTIR	: Fourier transform infrared spectroscopy
SEM	: Scanning electron microscope
MIT	: Molecular Imprinting Technology
NIP	: Non-Imprinted Polymer

LIST OF SYMBOLS

μL	: Microliter
μm	: Micrometre
mL	: Milliliter
mg	: Microgram
cm	: Centimetre
L	: Liter
V	: Volume
MW	: Molecular Weight
°C	: Celsius degree
eq	: Equation
M	: Molarity
k	: Selectivity coefficient
k'	: Relative selectivity coefficient
IF	: Imprinting Factor

1. INTRODUCTION

Plant sterols, also known as phytosterols, are an essential component of the membranes of all eukaryotic organisms and play an important role in their physiology. It is known that phytosterols have a variety of bioactive qualities that could affect human health. The most well-known property is the serum cholesterol lowering effect. It has been suggested that consuming a significant amount of phytosterols may reduce the absorption of cholesterol into the bloodstream and reduce the risk of cardiovascular, plant sterols are disorders and other diseases (Piironen et al., 2000.; Schaller, 2003)

Phytosterols are found in hard nuts, grains, seed, and vegetable oils. They are important due to their capacity to lower blood serum levels of LDL cholesterol, lower oxidative stress and cellular degradation, function as anti-inflammatory agents, and act as precursors for steroidal products used in the manufacture of various pharmaceuticals. In recent years, phytosterols have been referred to as biomedical research and bioactive compounds in pharmaceutical and pharmaceutical societies, which are naturally occurring in a wide range of interest (Hashim et al., 2014; Lindsey et al., 2003; Piironen et al., 2000; Schwarz et al., 2016).

Although it is possible to manufacture phytosteroids, they are difficult and expensive technically. Additionally, current techniques for extracting these compounds from plant extracts involve multiple stages and a variety of combinations, including crystallization, liquid-liquid or supercritical fluid extractions, and distillation (Fernandes & Cabral, 2007). In the analysis of natural phytosterol content of plant-based foods, it is necessary to establish fast, low-cost and reliable extraction techniques that can replace more time-consuming and labor-intensive standard sample extraction procedures. Molecularly imprinted polymers (MIPs) are viewed as a desirable solution for phytosterol isolation in this context. Due to these functional polymers can be used as reusable adsorbents for other classes of compounds in packed bed chromatography or solid-phase tank batch extraction. Solid phase extraction materials based on MIPs have recently advanced. MIPs are considered as the most potential artificial recognition materials by the reason of their low cost and high robustness (Bereli et al., 2020; Kamaruzaman et al., 2021).

Molecular imprinting is a contemporary technique for the synthesis of polymers with specific binding sites for the template molecule. Molecular imprinted polymers have been the focus of

research as a result of their molecular recognition features and are particularly interested in applications that require the binding and separation of specific molecular species. The chemical and mechanical durability of these polymers has made them crucial in a variety of sectors, from chromatography to assays, catalysis, sensor technologies, and controlled release systems. These polymers are also partially simple to manufacture and most of the chemical components can be imprinted. The purpose of the molecular imprinting technique is with the help of covalent or non-covalent interactions, functional monomers are arranged around a template molecule using the molecular imprinting technique. After that, the solids with chemical activity are produced using the right processing method. By removing the template molecule after the process, it is expected that an ideal material for processes such as chemical determination, catalysis and separation will be obtained by creating hollow regions in the structure that are specific to the template molecule. The molecular imprinting technique provides synthetically specific recognition sites in polymers. By using template molecules in this technique, polymers can be used for a long time without any change in their performance. In addition, they are materials with high reusability (Ramström & Mosbach, 1999; Vasapollo et al., 2011).

Application of MIPs in solid phase extraction (SPE) is incomplexed and basic to apply. Molecular imprinted polymer studies using selective solid phase extraction (SPE) media have come to the fore recently. Studies have shown that molecularly imprinted solid extraction procedures are the best ways to miniaturize SPE-based analytical chemistry techniques and provide selective extraction/pre-concentration when studying complicated samples (Jayasinghe & Moreda-Piñeiro, 2021).

The molecular imprinting technique is used as a synthetic recognition element in a variety of applications including diagnosis, purification, separation, food, environment, and health. This is one of its most significant benefits. Although many small molecules have been successfully imprinted in MIPs, some difficulties in imprinting large molecules such as proteins may still exist. Proteins have been polymerized in the past using techniques like epitope, surface (2D), and bulk (3D) printing (Cela-Pérez et al., 2013; Marjanovic et al., 2020; Shiomi et al., 2005; Wulff, 1995).

The binding capacity of MIPs is significantly influenced by morphology, which also affects enrichment effectiveness and detection sensitivity. Therefore, in the field of molecular

imprinting, morphological design and control are essential. MIP spheres are commonly utilized in sensor design, adsorption separation, and column filling because they are reusable and controlled (Rosengren et al., 2013). Monomers, template molecules, cross-linker, and a small amount of solvent are polymerized first to produce bulk polymers, and the polymers must be milled and sieved to produce irregular polymeric particles. The chromatography column and SPE column are then packaged with these polymeric particles. Bulk polymers have several advantages, including ease of preparation and high polymer yield. However, it had a few obvious shortcomings, such as low affinity binding sites after the procedure, low binding capacity due to large and irregular particle sizes. At this stage, the preparation of MIPs was important as it is a simple and highly repeatability monosize spherical structure. It is a simple, one-step polymerization process with a particle size suitable for SPE (Alizadeh & Memarbashi, 2012; Halhalli & Sellergren, 2015; Lu et al., 2020).

There have been many reported studies of cholesterol recognition based on molecular imprinted studies, but limited studies have been reported based on molecular stigmasterol (Stg) imprinting techniques as far as we know. Hashim et al investigated covalent and non-covalent imprinting techniques for the preparation of Stg imprinted polymers. In that study where they investigated the polymerization technique and showed that Stg was recovered at a good rate of 99%, they showed that the synthesized polymers could adsorb Stg 12.4 and 4 times more selectively than ergosterol and cholesterol molecules (Hashim et al., 2014).

Marjanovic et al reported Stg recognition via Stg imprinted polymers. MIP synthesis was carried out using toluene as a porogen solvent and Stg as a template molecule, in which precipitation polymerization was used. Imprinted and unimprinted polymers were characterized by SEM-EDS and FTIR. Adsorption studies were measured using UV-Vis. It has reported 0.040 mg/g Stg adsorption from synthetic medium, while the ability of MIP adsorption on Stg was 0.204 mg/g. All these studies show that MIP can be used as an adsorbent to adsorb Stg in real sample extracts, as the adsorption capacity of MIP against Stg molecule is better compared to NIP (Marjanovic et al., 2020).

Schwarz et al reported semi covalently imprinted polymers for Stg recognition. N,N′-dimethylacryl-amide (N,N′-DMAAM), the functional co-monomer used in hybrid semi-covalently imprinted polymers, demonstrated specific binding capacities ranging from 5.2 to

5.9 mg sterol/g MIP resin. MIPs prepared by non-covalent methods have significantly different binding properties and selectivity for phytosterol compounds compared to unprinted polymers (Schwarz et al., 2018).

In this thesis, we present a different technique for purification Stg from a plant sample. For this purpose, we aimed to prepared molecularly Stg-imprinted solid phase extraction polymers. The selectivity studies were conducted against cholesterol, ergosterol and Stg was determined from the plant sample.

2. LITERATURE REVIEW

2.1. Plant Sterols

Plant sterols are naturally occurring bioactive compounds that belong to the triterpene family. Plant sterols are substances found in plants that are chemically similar to cholesterol, except that an additional methyl or ethyl group is added (Moreau, Whitaker, & Hicks, 2002). Sterols exist in different forms in eukaryotic cells and are essential lipids for organisms. Phytosterols - land plant sterols and Cholesterols - animal sterols have very similar chemical structures (Gabay et al., 2010). Animals contain cholesterol, while plants contain sterol derivatives such as STG, β-sitosterol and campesterol, and the structures of both groups are very similar. These sterol derivatives mentioned are available as a mixture of sterols (Oka, Kiriyama, & Yoshida, 1973).

Plant sterols differ from cholesterol only in the structure of their side chain, with saturated sterols, called stanols, lacking the 5-double bond in their B-ring. Saturation of the most abundant plant sterol, sitosterol, results in sitostanol; saturation of campesterol results in campestanol (Figure 2.1).

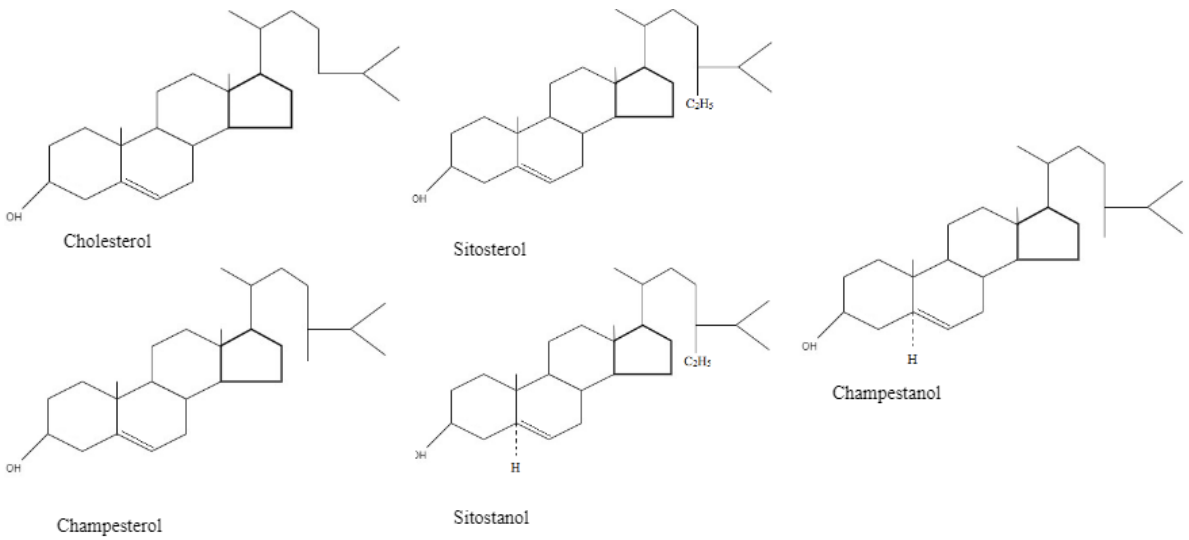

Figure 2.1. Chemical structures of cholesterol and some phytosterols.

The membranes of all plant cells contain phytosterols. It is especially rich in cereals and cereal product, fruits, vegetable oils and fats (Murkovic, Piironen, Lampi, Kraushofer, & Sontag, 2004). Phytosterols, free, esterified with fatty acids or conjugated with glycosides, occur naturally in plant and plant-based products (such as vegetables, fruits, seeds, vegetable oils, cereals and legumes) (Piironen et al., 2000). Phytosterols are found in vegetable oils in the form of free sterols or sterile esters of fatty acids (Verleyen et al., 2002). Furthermore, industrial wastes of soft and hard woods are also significant sources of phytosterols, as they contain 10 to 15% phytostanol. Phytostanols are fully saturated forms of phytosterols. It does not contain the carbon-carbon double bonds found in cholesterol and phytosterols (Moreau et al., 2002).

Phytosterols consist of 28 or 29 carbon atoms. They have points like cholesterol, which are their structural and functional properties. The majority of phytosterols have a side chain of nine to ten carbon atoms, while cholesterol has a side chain of eight carbon atoms. Over 200 types of phytosterols have been found in various plant species (Lagarda, García-Llatas, & Farré, 2006). Phytosterols have been shown to be highly effective in lowering serum cholesterol in addition to the risk of heart disease in humans. Phytosterols are also known to be important in the pharmaceutical, cosmetic, and nutritional industries. It is widely used in the food and cosmetics industries due to its health benefits (Rudkowska, 2010). Figure 2.2 shows the effects of phytosterols on human health.

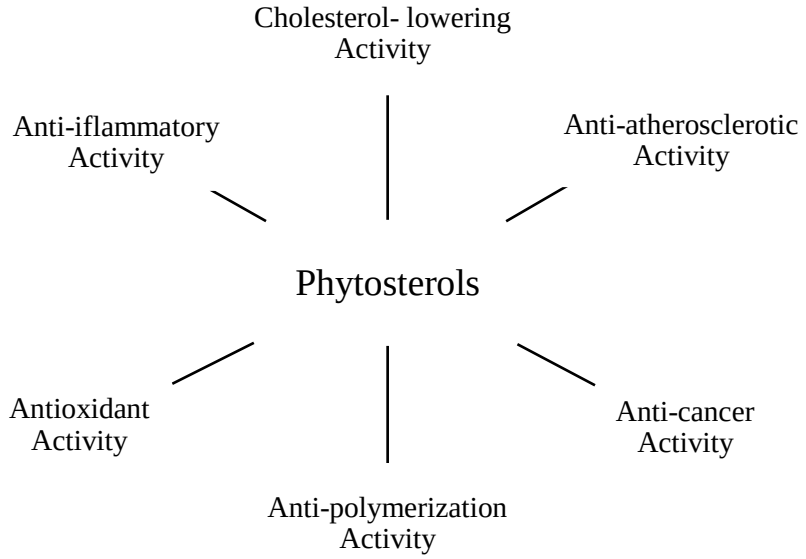

Figure 2.2. Effects of phytosterols on human health.

2.1.1. Stigmasterol

Stigmasterol (Stg) is an unsaturated plant sterol also referred to as Stigmasterin or Wulzen anti-stiffness factor. Rosalind Wulzen, a physiologist at the University of California, discovered Stg in a variety of medicinal plants. Adolf Wind Form and A. Hauth isolated it for the first time in 1906 in Calabarbohne, and it was later isolated from various medicinal plants (Kaur, Chaudhary, Jain, & Kishore, 2011). Stg is used in a variety of chemical processes that produce a wide range of synthetic and semi-synthetic compounds for the pharmaceutical industry. It serves as a precursor in the synthesis of progesterone and is known to act as an intermediate in the synthesis of some products -such as corticoids, androgens, estrogens, and vitamin D3 (Sundararaman & Djerassi, 1977). Stg is a plant lipid that is very close to cholesterol in chemical structure (Salehi et al., 2020).

Plants produce sterol mixtures containing sitosterol, Stg, campesterol and cholesterol. Animals and fungi cannot do this process. Sterols help maintain the plant cell's plasma membrane fluidity and permeability, under stress conditions (Hartmann, 1998). Stg is essential for the production of hormones such as progesterone, estrogens, androgens and corticoids. Furthermore, lots of studies have shown that Stg can inhibit the alpha-amylase enzyme, and its bioactivity has pharmacological effects such as antidiabetic, hypoglycemic, antiosteoarthritic, antimutagenic, cytotoxicity, anti-inflammatory, and antioxidant (Kaur et al., 2011; Kumar, Kumar, & Prakash, 2013; J. Wang et al., 2017). It has also been shown in several studies that it can inhibit the growth of tumors. Therefore, this steroid derivative can also be used as a potential drug in the treatment of various diseases (Ali et al., 2015; Kangsamaksin et al., 2017).

Stg reduced amyloid-β-peptide (Aβ) secretion strongly by pleiotropic mechanisms in human neuroblastoma cells SH-SY5Y. Aβ secretion was raised via cholesterol, β-sitosterol, brassicasterol and campesterol (MS et al., 2018). In addition, Stg had stronger antagonist activity against the nuclear bile acid receptor (Carter et al., 2007). In comparison to sitosterol and campesterol, Stg was found to have the highest binding affinity for the enzyme cyclooxygenase (COX-2) (Afroz et al., 2019).

2.1.2. Biosynthesis Of Stigmasterol

Stg is one of the significant phytosterol that is found in plant cell membranes which has not been shown to be a membrane reinforcer (Krajewski-Bertrand, Milon, & Hartmann, 1992; Schuler et al., 1991). It has recently been suggested that the isoprene building blocks of phytosterols are derived biosynthetically from the mevalonate pathway.

When the mevalonate and deoxyxylulose mechanisms for producing phytosterols were investigated in one study using callus leaf explant cultures of Croton sublyratus, It was discovered that biosynthesis took place during the culture's linear phase, and both channels contributed equally (De-Eknamkul & Potduang, 2003). After a series of enzyme-catalyzed reactions that result in the formation of 2,3-oxidosqualene, Stg is produced in the mevalonate pathway (Schaller, 2003).

2.1.3. Chemical Structure Of Stigmasterol

Stg is a member of the group of plant sterols that are chemically similar to cholesterol. When Stg ($C_{29}H_{48}O$) and cholesterol ($C_{27}H_{46}O$) are compared structurally, Stg has an extra ethyl group and a double bond in the side chain (Harborne, 1998). Stg is a stereolipid with an ethyl group at the C24 carbon atom. It also has the skeleton of a stigmastan. It is hydrophobic and mostly neutral. Among plant sterols, Stg is one of the most prevalent. Its primary function is to maintain the physiology and structure of the cell.

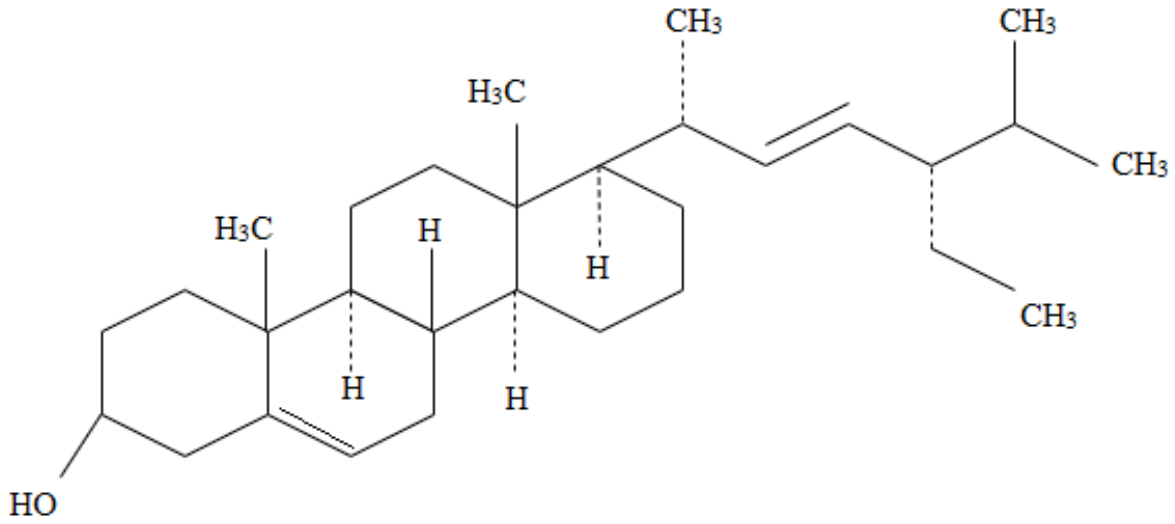

Figure 2.3. Chemical structure of stigmasterol

Stg is a steroid derivative characterized by the hydroxyl group in position C-3 of the steroid skeleton, and unsaturated bonds in position 5-6 of the B ring, and position 22-23 in the alkyl substituent. Cholesterol and Stg are structurally very similar, only differing in their side alkyl chain. According to the study of Lengyel et. al. (2012), similar susceptibility to oxidation is expected for their 5, 6 and 7 ring-positions. In addition, a variety of factors other than thermodynamics could be involved in the differential oxysterol formation from cholesterol compared to Stg (Barriuso, Ansorena, Poyato, & Astiasarán, 2015; Lengyel et al., 2012).

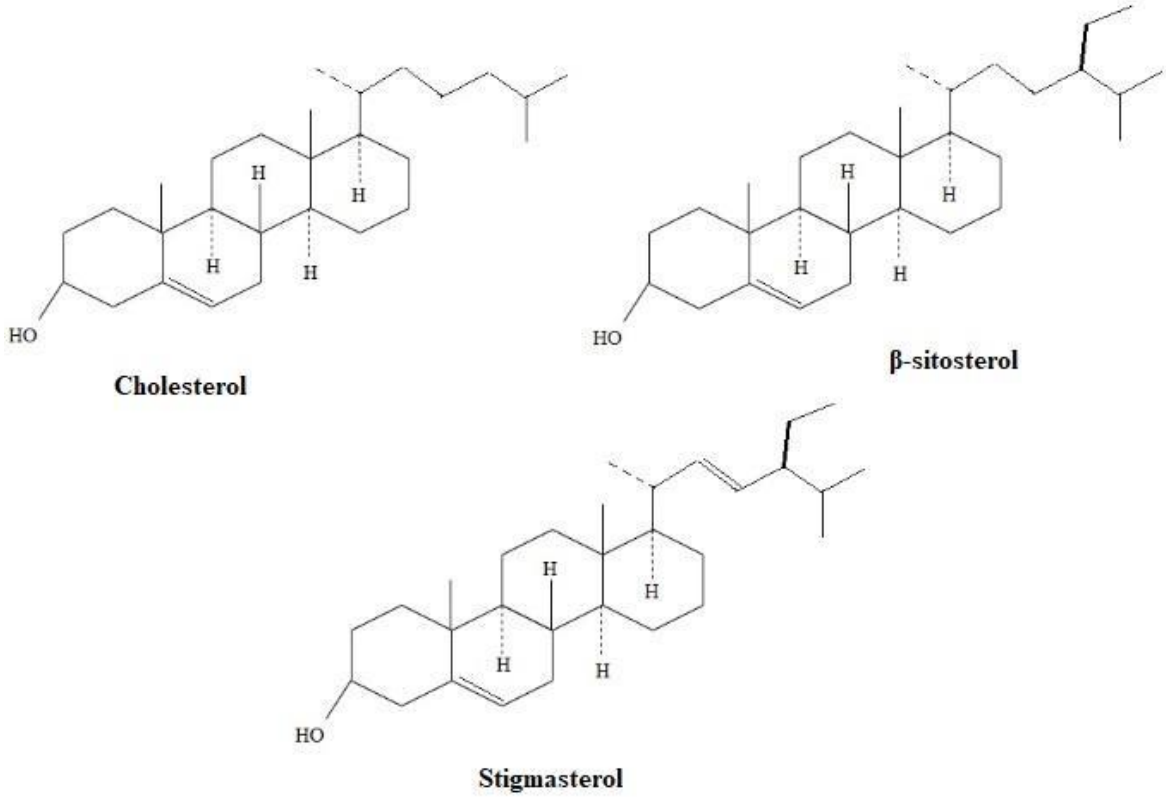

Figure 2.4. Molecular models for cholesterol, β-sitosterol and stigmasterol.

2.1.4. Clinical Significance Of Stigmasterol

Stg is a significant sterol found in plant cell plasma membranes and is associated with cell growth (Hartmann, 1998) and activation of plasma membrane H+-ATPase (Grandmougin-Ferjani, Schuler-Muller, & Hartmann, 1997). Stg, one of the many valuable compounds, has been isolated from numerous plants and studied for a variety of pharmacological and biological activities such as anti-inflammatory, anti-osteoarthritic, anti-oxidant and anti-hypercholesterolemic.

Anti-inflammatory Activity: The anti-inflammatory properties of Stg were examined in a study by Khan et al. on rats to treat rheumatoid arthritis (RA), which is brought on by increased proinflammatory cytokine production. Stg treatment was found to significantly reduce the expression of proinflammatory mediators like iNOS, IL-6, IL-1, COX-2, and TNF- and increase the expression of anti-inflammatory cytokines like IL-10 (Ahmad Khan et al., 2020). In a different study, the effect of Stg on oxidative stress, inflammatory cell proliferation, lung histopathology and remodeling was examined. Significant antiasthmatic activities were present

in Stg, and it had suppressive effects on important symptoms of allergen-induced asthma (Antwi, Obiri, & Osafo, 2017).

Anti-osteoarthritic Activity: Gabay investigated the anti-osteoarthritic activity of Stg in a study (Gabay et al., 2010). In this study, newborn mouse chondrocytes and human osteoarthritis (OA) chondrocytes were stimulated with or without IL-1b for 18 hours before being incubated with Stg for 48 hours. After 18 hours of IL-1beta treatment, the expression of several genes involved in cartilage remodeling increased, and as a result of the study, Stg was found to have an anti-osteoarthritic effect by significantly reducing this effect (Gabay et al., 2010).

Antioxidant Activity: In the study in which the neurological deficiencies of rats were analyzed, it was observed that Stg protected the brain from I/R damage by reducing oxidative stress and inflammation (Liang et al., 2020). In another study, the antioxidant property of Stg isolated from Butea monosperma bark was investigated and an increase in catalase (CAT), glutathione (GSH) and superoxide dismutase (SOD) activities, and a decrease in hepatic lipid peroxidation (LPO) were observed (Panda et al., 2009).

Anti-hypercholesterolemic activity: Studies have shown that Stg has a significant effect on serum cholesterol comparable to the antihypercholesterolemic activity of β-sitosterol. It has been noted that plant sterol competes with cholesterol for intestinal absorption, reducing the plasma levels of cholesterol. In a study, Stg inhibited the production of cholesterol by blocking the enzyme sterol-24 reductase in human Caco-2 and HL-60 cell lines. Stg has been shown to reduce plasma cholesterol levels, inhibit intestinal cholesterol and plant sterol absorption. It has been revealed as a result of research that it suppresses hepatic cholesterol and classical bile acid synthesis (Batta et al., 2006).

2.2. Affinity Chromatography Techniques

Affinity chromatography is a type of liquid chromatography that uses biologically similar interactions to separate and specifically analyse sample constituents. Affinity chromatography is an effective and powerful technique for isolating and purification the several essential biomolecules such as antigens, antibodies and enzymes (Gu, Hsu, & Syu, 2003).

Affinity chromatography technique manages reversible biospecific binding between biomolecules and immobilized ligands. This affinity chromatography technique achieves selective purification of enzymes. Another important application of affinity chromatography is the efficient isolation of enzymes in purification processes. It provides that enzyme activity losses are kept to a minimum in multi-stage purification processes. Affinity chromatography is widely used in biomolecule preparation and separation. As a result, this separation technique is becoming increasingly important (Hage et al., 2012).

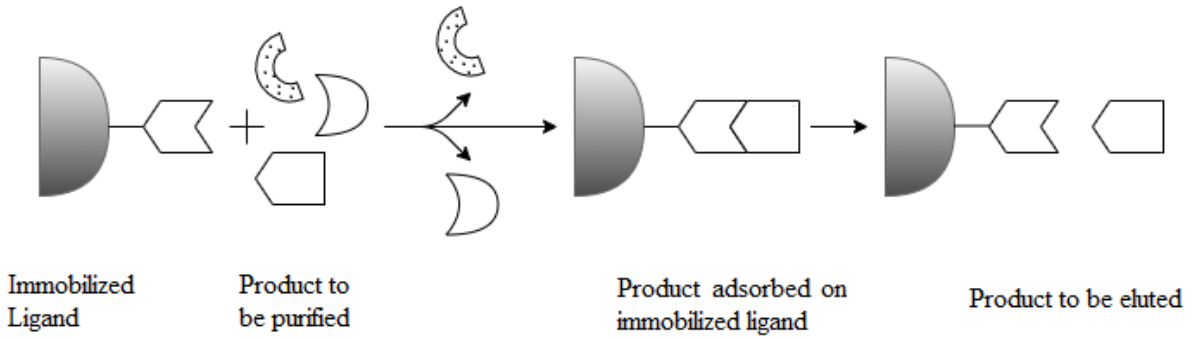

Figure 2.5. Principle of affinity chromatography.

2.2.1. Solid Phase Extraction

Solid-phase extraction (SPE) is a widely used sample preparation technique that can be applied directly to gas-solid-phase and liquid-solid-phase samples or indirectly to solid samples by means of, for example, thermodesorption followed by chromatographic analysis (Płotka-Wasylka, Marć, Szczepańska, & Namieśnik, 2017).

The analysis steps of the SPE method are basically based on the principle of filling small, disposable extraction columns or discs with various holding agents and passing the liquid

samples through the columns and discs prepared to separate (clean) the unwanted components, condense and further change the sample matrix structure. The primary goals of such treatments are to remove matrix components and enrich the analyte in the sample. Otherwise, they can slow down detection time and even cause equipment damage (Ścigalski & Kosobucki, 2020).

Among the most commonly used sample preparation techniques are solid-phase micro-extraction (SPME), matrix solid-phase dispersion (MSPD), stir bar sorptive extraction (SBSE), and ion-exchange solid-phase extraction (IE-SPE). These solid phase extraction techniques reduce matrix effects while increasing sensitivity and reproducibility in selective sample preparation.

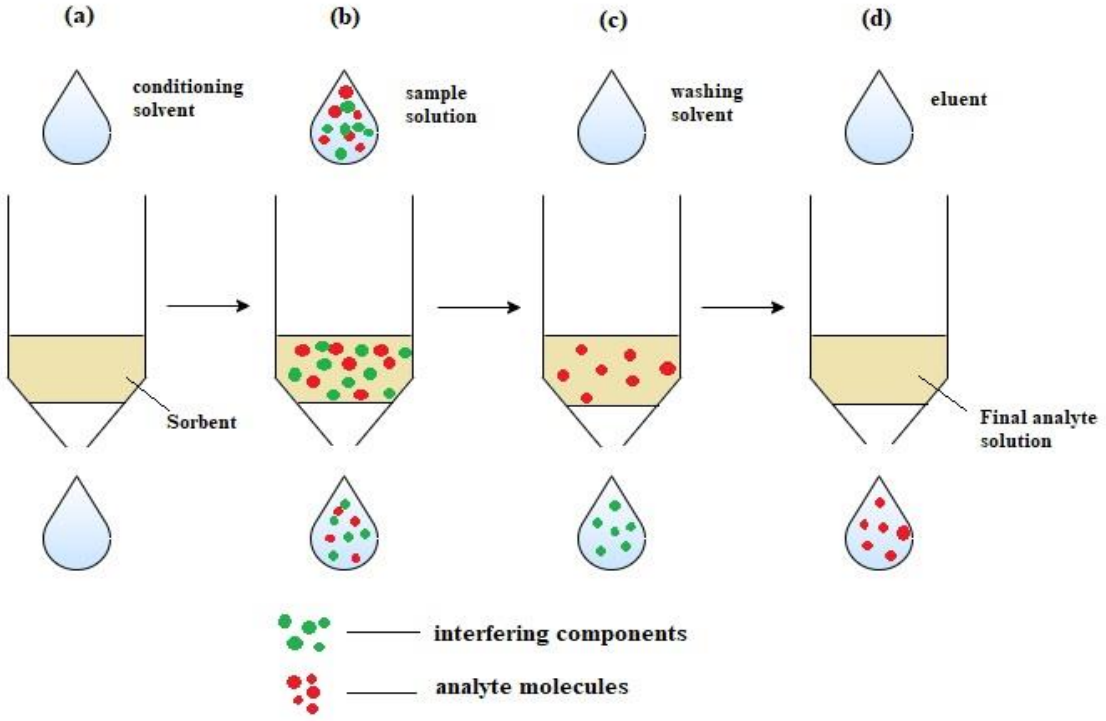

Figure 2.6. The basic procedure of SPE method. (a) conditioning, (b) sample loading, (c) rinsing, (d) elution.

In the literature, there are many separation and pre-concentration methods for various purposes. Liquid-liquid extraction (solvent extraction), ion exchange, electrodeposition, and membrane filtration are some of the examples generally used for this purpose. Matrix removal (separation),

trace enrichment (preconcentration) and medium exchange are the major goals of SPE (Alexander et al., 2006; Liška, 2000).

In a study by A. R. Koohpaei et al., solid phase extraction has been shown to be one of the major applications of molecularly imprinted polymer domains for cleaning environmental and biological samples. In terms of critical factors, solid phase extraction of a triazine herbicide called atrazine using imprinted polymer was optimized by an experimental design approach. Factors affecting the efficiency of molecular imprinted solid phase extraction such as pH, concentration, flow rate, volume, elution solvent, wash solvent and sorbent mass were investigated. Chemometry is frequently used in the optimization of analytical methods. The central composite design is thought to help improve solid phase extraction in molecularly imprinted polymers (Koohpaei et al., 2008).

2.2.2. Mono-sized Spherical Particles

The binding capacity of MIPs, as well as their effectiveness and detection sensitivity, are significantly influenced by their morphology. The preparation technique and morphology have an impact on the diameter and size of the MIP particles. Over time, MIPs' morphology changed from irregular particles to organized spheres and hierarchical structures (Alizadeh & Memarbashi, 2012; Halhalli & Sellergren, 2015).

There has been significant progress in the development of MIPs with various morphologies in recent years. Several methods for producing MIPs with the desired shape, size, and particle size distribution have been developed. MIPs with many spherical, porous, hollow, core-shell shapes, including packed columns and chemical sensors, have been successfully prepared (Lu et al., 2020). MIP microspheres have good dispersion and are generally spherical with particle sizes of about ten microns. MIP spheres are widely used in column packing, adsorptive separation, and sensor construction because they are replaceable and controllable (Giovannoli et al., 2015; Shen & Ye, 2011; D. Wang, Hong, Yang, & Row, 2003).

2.3. Molecularly Imprinted Technology

High selectivity and specificity receptors are created using a technique called molecularly imprinting technology (MIT). It is an excellent method for a specific analyte that can be used in a variety of applications. This technology is now a sustainable synthetic approach for creating strong molecular recognition materials capable of imitating natural recognition entities like antibodies and biological receptors (Vasapollo et al., 2011).

A functional monomer and an analyte (template) combine to generate a three-dimensional polymer complex when cross-linking agents are present. The template is removed from the polymer after polymerization. Certain recognition sites are obtained based on the size, shape, and functionality of the template molecule. Intermolecular interactions between the template molecule and the functional groups contained in the polymer matrix, such as hydrogen bonds, dipole-dipole interactions, and ionic interactions. As a result, polymers with only the template molecule recognition region are obtained. (Ramström & Mosbach, 1999).

2.3.1. Molecularly Imprinted Polymers

There are many applications for molecular imprinted polymers (MIPs), such as biosensor design, catalysis and chromatography. Molecular imprinting technique basically occurs in three steps. Firstly, the monomer carrying the functional group or groups interacts covalently or noncovalently with the template molecule to generate a pre-complex.

In the second step, the polymerization process is initiated with the help of this pre-complex, a suitable cross-linker and polymer initiator. Finally, the imprinted polymer is washed with a suitable solvent and/or solvent system to remove the template molecule in the structure. A highly selective polymeric structure is obtained that recognizes the three-dimensional chemical structure of the template molecule, namely the analyte (Orozco et al., 2013; Soysal et al., 2013; Tang et al., 2016). Schematically this can be represented by Figure 2.7.

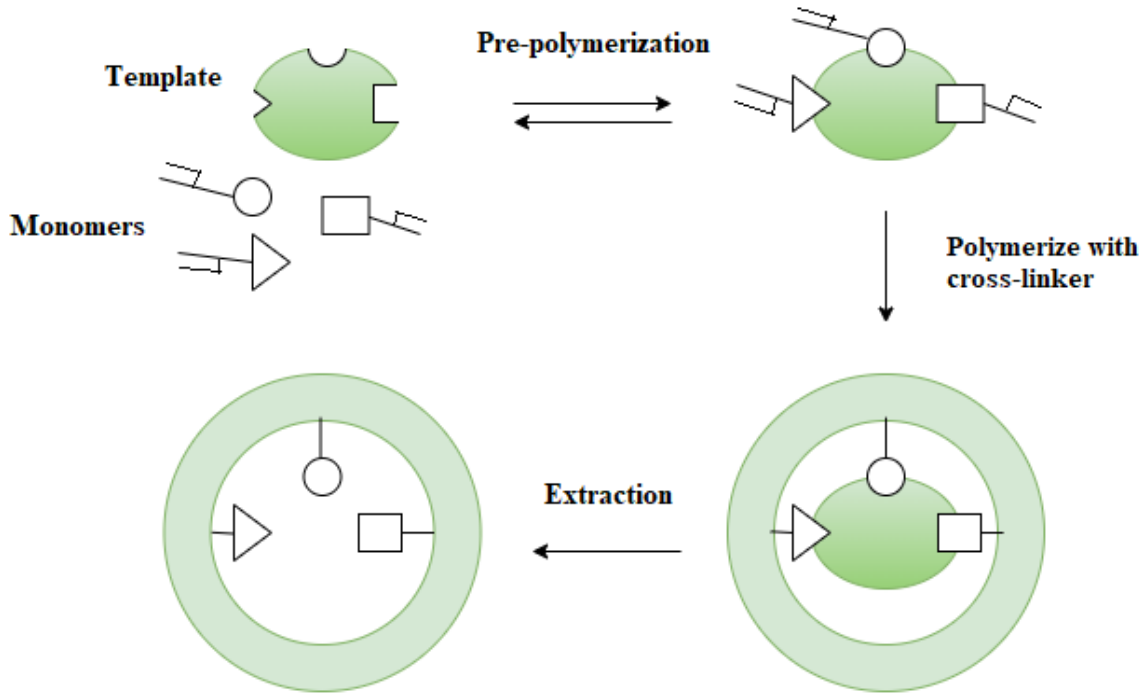

Figure 2.7. Representative illustration of molecular imprinting technique.

Pre-polymerization, polymerization around pre-complex, removal of the template molecule and formation of template-specific cavities.

Molecular imprinted polymers with specific binding sites are frequently used in many analytical applications due to their high specificity, easy preparation, and being physically and chemically resistant materials. Solid phase extraction (Demirkurt, Olcer, Demir, & Eroglu, 2018; Garcia et al., 2018), chromatography (Bayram et al., 2017) catalytic and sensor (Zhang et al., 2018) studies on the use of molecular imprinted polymers in analytical techniques seem to have been on a rapid rise since the 2000s.

2.3.1.1. Covalent Imprinting

Before polymerization, a powerful and reversible covalent imprinting occurs between the monomers that will be imprinted. After the polymerization process, the covalent bonds are broken, and the mold is removed from the polymer. When the target molecule comes into

contact with the polymer, the covalent bond is reformed. One benefit of this method is that functional groups are only associated with the template site. However, at this stage, only a limited quantity of compounds can be printed. Although a covalent approach is stronger between the ligand and the matrix, non-covalent approaches are preferred in most cases, as this is often costly in terms of compatibility and binding kinetics.

2.3.1.2. Non-Covalent Imprinting

Noncovalent interactions, such as H-bonding, ion pairing, and dipole-dipole interactions, are used in non-covalent imprinting to bind the functional monomer to the template molecule. After polymerization, the template molecule is removed from the polymer with suitable solvents. Imprinted polymers with template molecules are bonded by non-covalent interactions. This method was first introduced by Mosbach's group with organic polymers. Due to its simplicity, this method is the most commonly used method for the preparation of molecular imprinted polymers. Many commercially available functional monomers have been reported in studies (Alexander et al., 2006; Ramström & Mosbach, 1999).

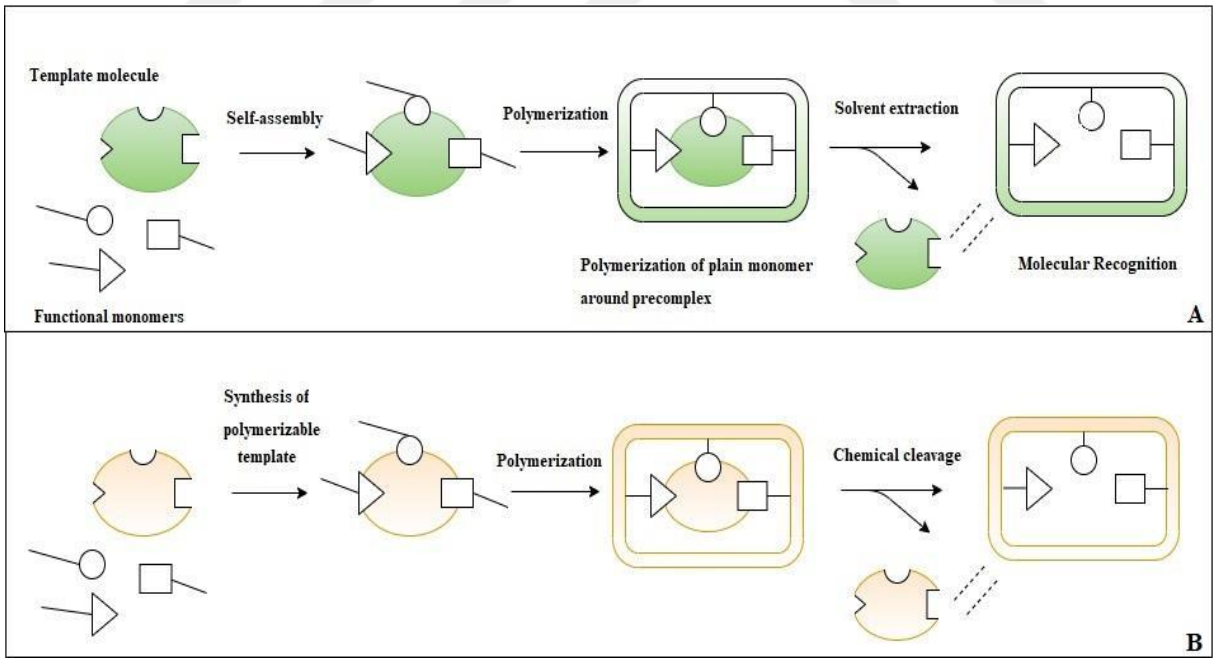

Figure 2.8. Molecular Imprinting Approaches. A) Non-covalent, B) Covalent imprinting.

2.3.2. Polymerization

Free radical polymerization is generally used in the preparation of MIPs, with azo initiators being the most commonly used materials. The synthesis is typically carried out under mild reaction conditions with a variety of functional groups and template structures. Typically, polymerization reactions happen quite quickly. Azo-N-N'-bis-isobutyronitrile is one of the most popular azo initiators (AIBN). AIBN can be used as a source of free radicals by photochemical or thermal degradation occurs at 40°C, while thermal degradation occurs above this temperature. The monomer-template complex is polymerized over the functional monomer using a suitable cross-linker and initiator.

2.3.2.1. Template Molecule

Template molecules have a significant function and act as a target compound in analytical reactions. Its primary function is to regulate functional groups attached to monomers. As a result, an ideal template molecule should be inert during polymerization. If the template can participate in radical reactions or is otherwise unstable under polymerization conditions, alternative imprinting strategies may be required. An ideal template molecule contains no groups that participate in or hinder polymerization, is chemically stable during the polymerization process. It has functional groups that combine well with functional monomers.

2.3.2.2. Monomers

The functional monomer is assigned by functional groups, which can form a complex with the template molecule via covalent or non-covalent interactions. Copolymerization with the cross-linked monomers holds the monomers in place temporarily around the template. Because the formation of a stable template monomer complex is required for molecular recognition, the functional monomers are selected to interact with the template. Copolymerization with cross-linking monomers fixes the position of the monomers in space around the template. Methacrylic acid (MAA), acrylic acid (AA), 2- or 4-vinylpyridine (2- or 4-VP), acrylamide, trifluoromethacrylic acid and 2-hydroxyethyl methacrylate (HEMA) are most common used monomers in molecular imprinting technology. These are shown in Figure 2.9.

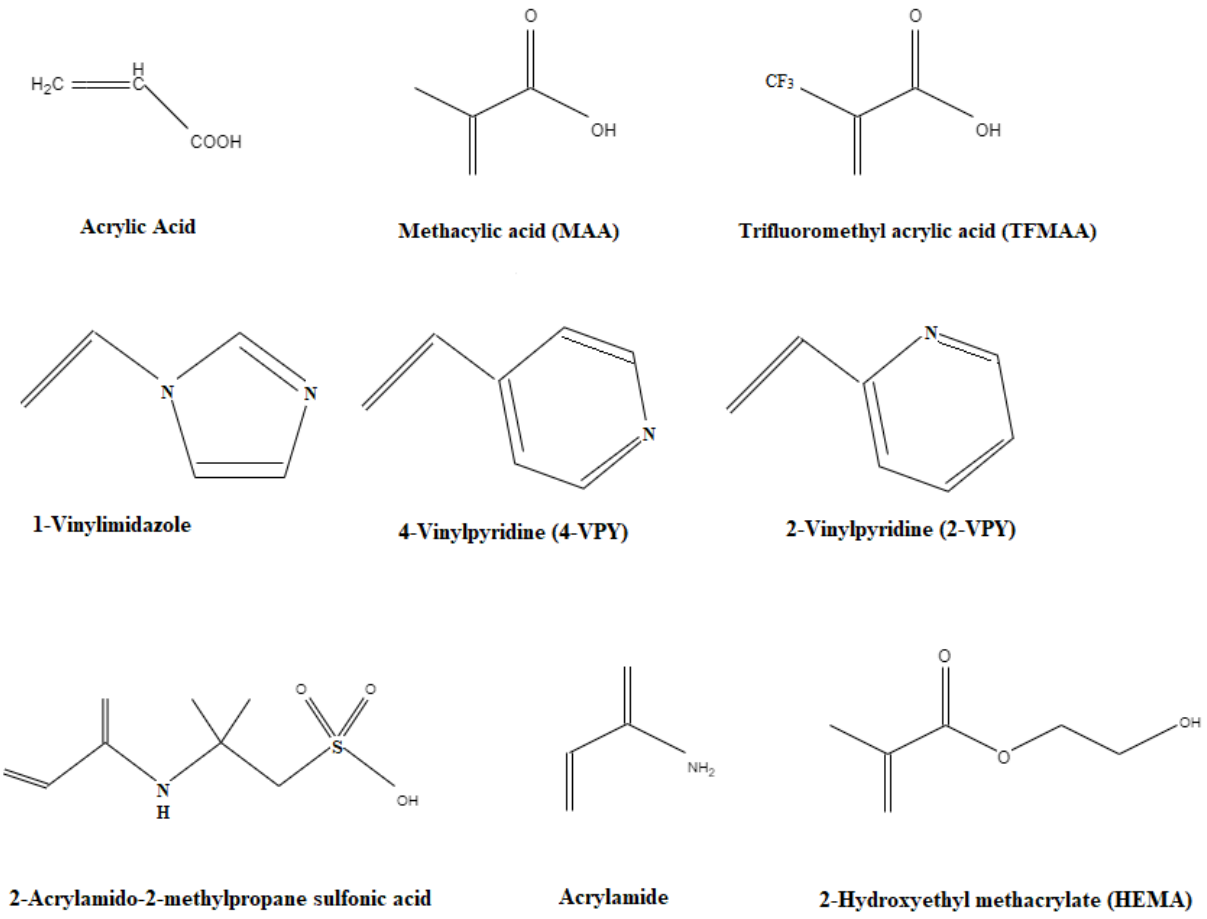

Figure 2.9. Monomers used in molecular imprinting method and their chemical structures.

2.3.2.3. Cross-linker

Cross-linkers are provided that primarily control the morphology of the imprinted polymer matrix, the stability of the binding moieties of the imprinted molecule or ion, and the high mechanical stability of the polymer matrix. Cross-linkers attach the functional groups of functional monomers to imprinted molecules, resulting in a highly cross-linked rigid polymer. The functional monomer must be thoughtfully chosen to ensure complementary interactions with the template and substrates.

The most commonly used cross-linkers in research are ethylene glycol dimethacrylate (EGDMA), divinylbenzene (DVB), N,N-methylenebisacrylamide (MBAA) and

trimethylolpropane trimethacrylate (TRIM). The structures of various cross-linkers are shown in Figure 2.10. The high cross-linking ratios are usually preferred in order to obtain permanently porous (macroporous) materials and to be able to produce materials with sufficient mechanical stability. Consequently, the amount of cross-linker used should be sufficient to keep the recognition sites stable. There are several cross-linkers known to be compatible with molecular imprinting. Some form complexes with the template; some act as functional monomers.

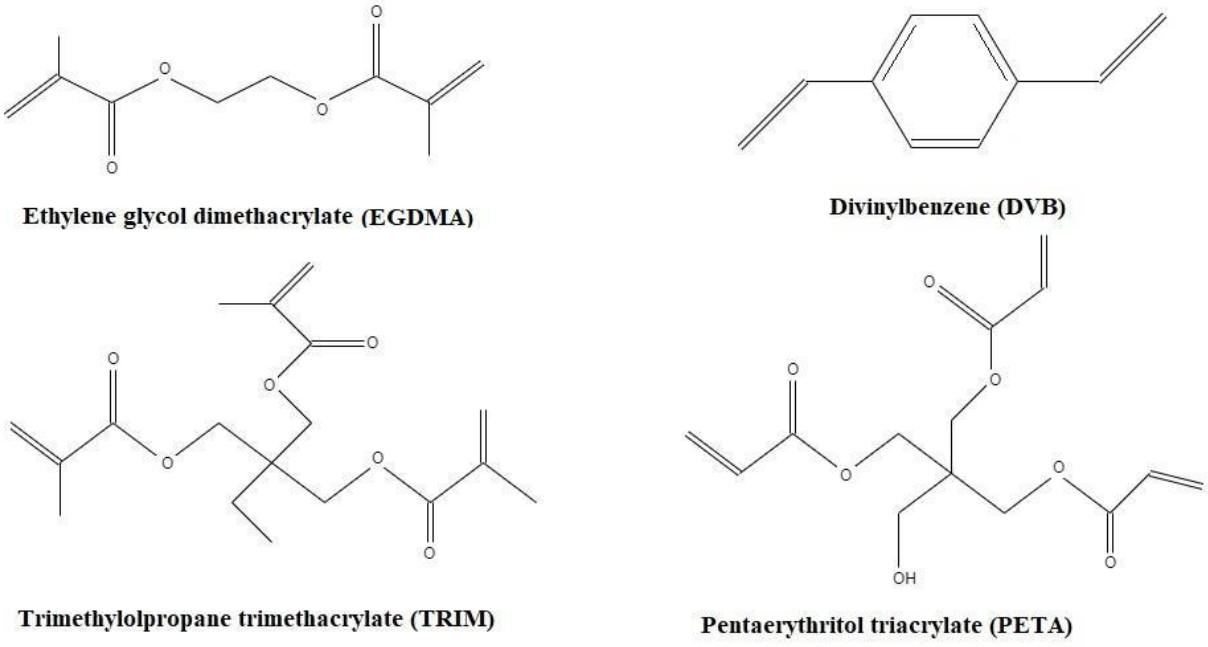

Figure 2.10. The chemical structures of cross-linkers used in molecular imprinting method.

2.3.2.4. Solvents

The porous structure of MIP, also known as macroporous polymers, is generated by the porogenic solvent. It also impacts the bond strength between functional monomers and templates, as well as the polymer's characteristics and morphology, particularly in non-covalent interaction systems.

The template molecule, the initiator, the monomer, and the cross-linker must first be soluble in the porogenic solvents. Second, the porogenic solvents should create large pores to ensure that the resulting polymer has good flow properties. Third, because the monomer is critical for MIP

selectivity, relatively low polarity porogenic solvents should be used to minimize interference during complex formation between the imprinted template and the monomer. Non polar and aprotic solvents such as toluene and chloroform are preferred; water or protic solvents may be used if hydrophilic forces are involved in complex formation.

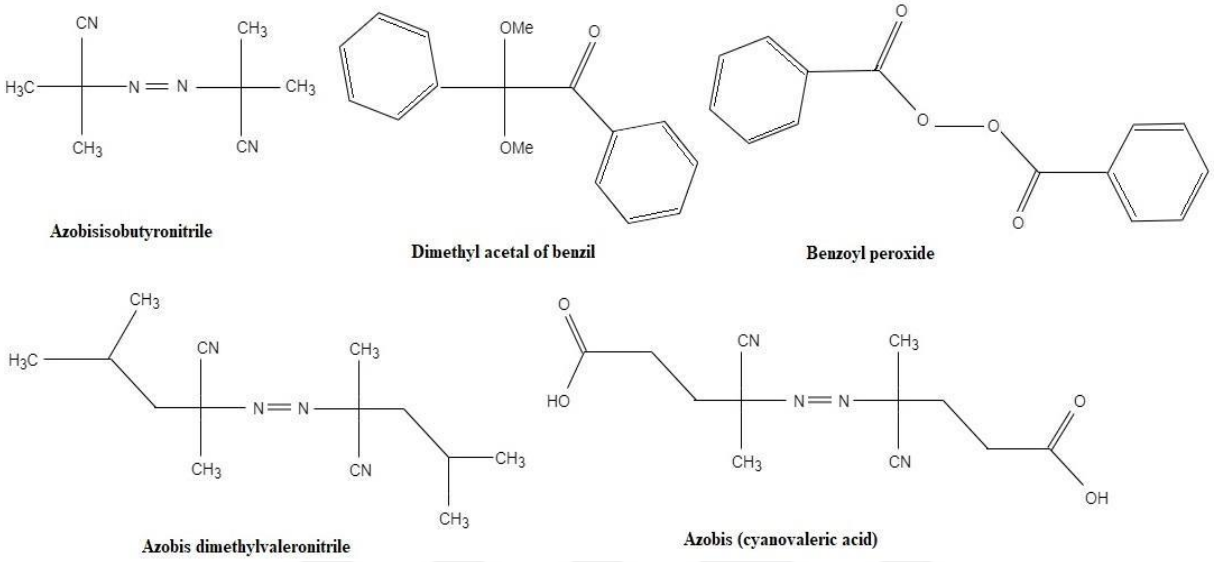

Figure 2.11. The chemical structures of non-covalent molecular imprinting initiators.

It has been shown in many studies that the polymerization of MIP at low temperatures has more selectivity than polymers prepared at higher temperatures. Furthermore, high temperatures are damaging to complex stability. The reproducibility of monolithic stationary phases is thereby reduced. It can also cause large falls in column pressure. Mosbach et al., for instance, published a research on the enantioselectivity of l-PheNHPh-terminated polymers, one of which was thermally polymerized at 60°C and the other photochemically polymerized at 0°C. The results showed that better selectivity was obtained at the lower temperature than the identical thermally polymerized polymers. The reason for this was again postulated based on the Le Chatelier principle, which predicts that lower temperatures drive the prepolymer complex to form complexes, thereby increasing the number and possibly the quality of the binding sites formed (al Shannaq & Farid, 2015; Kempe & Mosbach, 1995; Yan & Kyung, 2006).

2.4. Polymerization Synthesis Techniques

Polymerization is the formation of a macromolecule by combining small molecules called monomers. Because this macromolecule is a polymer, monomers serve as polymer building blocks. These polymers can be created in a variety of ways. Some of these methods include suspension polymerization and emulsion polymerization.

2.4.1. Suspension Polymerization

Suspension polymerization is a polymerization method that belongs to encapsulation processes. This process is used to make many commercial resins such as polystyrene, polyvinyl chloride (PVC), and poly(methyl methacrylate). In general, what is found in a suspension polymerization system is as follows: monomers, stabilizing agents, dispersion medium and soluble initiator. The monomer must be highly insoluble in order to be dissolved in water. Prepolymers or partially polymerized monomers can be used if the monomer is not adequately dissolvable. These polymers are either water insoluble or have much lower solubility than monomers. During the polymerization, the suspension must be sufficiently stirred and stabilized, or the particles will agglomerate and form a large mass. The final polymeric particles range in size from 0.1 to 5 mm in diameter (al Shannaq & Farid, 2015).

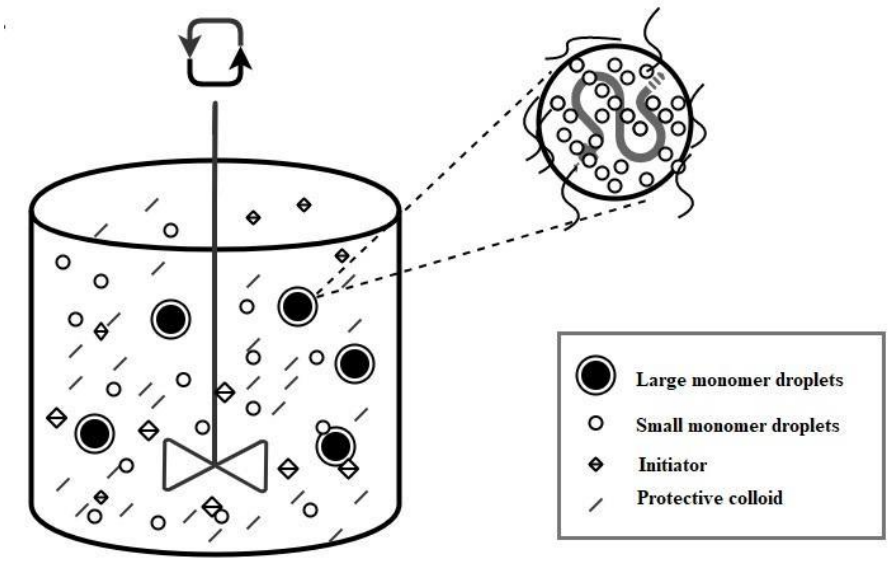

Figure 2.12. Production of microcapsules by suspension polymerization. Emulsion Polymerization

2.4.2. Emulsion Polymerization

Emulsion polymerization is a crucial process for the polymerization of a wide range of monomers. vinyl acetate, acrylates, methacrylates, acrylamide, vinyl chloride and chloroprene are examples of monomers. It's also used to make copolymers such as acrylonitrile butadiene styrene (ABS). Emulsion polymerization is a type of polymerization that happens most commonly in emulsions. Water, monomers, an initiator, and a surfactant are all that is required.

The polymerization mechanism in the emulsion polymerization process is much more complex, the products also differ from one another in terms of their properties. While the product particle size in the slurry process is in the range from 10 μm to 10 mm, the emulsion polymerization produces significantly smaller polymeric particles with 0.05 to 5 μm. The resulting product is an artificial latex.

One of the important technical advantages of emulsion polymerization is that it is faster compared to other polymerizations. The main difference between suspension and emulsion polymerization is that in suspension polymerization a mechanical mixing is required whereas in emulsion polymerization it is not needed. In summary, emulsion polymerization requires the use of water, a monomer, an initiator, and a surfactant; suspension polymerization requires the use of a dispersion medium, monomers, stabilizers, and initiators. Finally, the final products of emulsion polymerization do not require any modification. However, in suspension polymerization, the situation is the opposite. The reason for this is that the final products exist in the liquid medium as a suspended sphere (Cunningham et al., 2014; Hood et al., 2014).

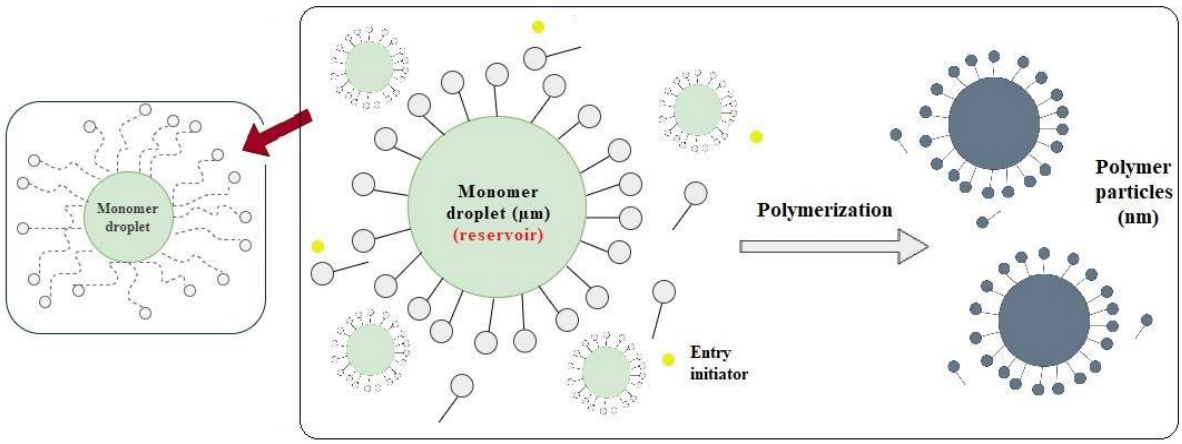

Figure 2.13. Emulsion polymerization process.

3. MATERIALS AND METHODS

3.1. Materials

Stigmasterol (Stg), Divinylbenzene-80 (DVB-80), 4-vinylbenzoic acid (VBA), methacrylic acid (MAA) and 2,2-azo-bis-isobutyronitrile (AIBN) were purchased from from Sigma-Aldrich (St. Louis, MO, USA). All chemicals, including acetonitrile, methanol, and ethanol, were purchased from Sigma-Aldrich (St. Louis, MO, USA). The necessary solutions were made using analytical-grade reagents, and clean water with a resistivity of 18 M-cm at room temperature. All reagents were stored in accordance with the given instructions and waste was disposed of in accordance with the rules.

Chemicals and samples were weighed using Shimadzu Type ATX224 Electronic Balance. Biobase Type MX-T6-S Rotator was used to mix the prepared samples homogeneously. Model of Millipore DIRECT-Q3 UV water device with a filter was used for the water system. Solid phase from the sample was separated by Beckman Coulter Type Allegra X-30R Centrifuge device. Roller Vortex (MX-T6-S, Biobase, China) was used to mix solutions. Uv-Vis Spectrophotometer (Genesys 150, Thermo Scientific, United States) was used to determine the adsorption capacity, selectivity and many other characteristics of the polymer. The surface morphology and chemical properties of the synthesized polymers were evaluated with Scanning Electron Microscopy (SEM) (FEI, Quanta 650 Field Emission SEM, USA) and Fourier Transform Infrared Spectroscopy (FTIR) (Jasco, FT/IR-6700, USA) devices, respectively.

3.2. Preparation of Stigmasterol-MIP and NIPs

Stg-imprinted monosize solid phase extraction spheres (Stg-MIPs) and NIPs were made using Stg as the template molecule, 4-vinylbenzoic acid (VBA) as the functional monomer, methacrylic acid (MAA) as the monomer, divinylbenzene-80 (DVB-80) as the cross-linker, and 2,2’-azobisisobutyronitrile (AIBN) as the initiator in a solution of acetonitrile/toluene as the porogen (3/1, v/v).

Table 3.1. Recipe for polymer synthesis and polymerization circumstances.

Chemicals	**Amount of Chemicals**
Stigmasterol	(0.23 mmol) 95 mg
VBA	(0.46 mmol) 67.79 mg
MAA	(0.68 mmol) 58 µL
DVB-80	(3.40 mmol) 484 µL
AIBN Acetonitrile/Toluene (3/1, v/v)	(0,25 mmol) 41.05 mg (9.375 mL/3,125 mL)
Polymerization Conditions: Temperature: 60 °C, Time: 24 hours	

Batch polymerization method was preferred for the preparation of Stg-MIPs and NIPs. First, Stg (0.23 mmol) was dissolved in acetonitrile/toluene solution and then VBA functional monomer (0.46 mmol) was dissolved in this solution to have Stg-VBA pre-complex in 1:2 molar ratio and interacted for 4 hours at 4 °C. Polymerization was carried out for 24 hours at 60 °C using MAA (0.68 mmol), DVB-80 (3.40 mmol), AIBN (0.25 mmol), and acetonitrile/toluene (75/25 v/v, 12.5 mL) solution in addition to the Stg-VBA pre-complex. NIPs were synthesized by the same Stg-MIPs preparation procedure without using Stg molecules. The reaction mixture acquired a milky look at this point. Centrifugation was used to separate the supernatants from the reaction medium, and the sedimented polymers were then added to the solid part. The polymers, all of which were dried at 40°C overnight and weighed on analytical balance (m_{dry}).

3.3. Template Removal

The polymers were washed with a methanol/acetic acid (9/1, v/v) solution to remove the template molecule from the synthesized Stg-MIPs. The removed Stg was determined after each elution by making absorbance measurements at 205 nm wavelength with a UV spectrophotometer. Up till there was no more Stg, this process was done numerous times. As a result of the template removal, specific cavities for Stg were revealed.

3.4. Characterization Studies

Swelling ratio of synthesized polymers was determined by swelling test. Scanning electron microscopy (SEM) was used to analyze the morphological structures and particle sizes of these materials. The characterization of the chemical structures was done by Fourier transform infrared spectroscopy (FTIR) (Jasco, FT/IR-6700, USA) method.

3.4.1. Swelling Tests

The swelling ratio of the microspheres obtained by polymerization was determined in distilled water using the gravimetric method. For this, dry spheres were placed in a cylindrical glass tube. The height of the uninflated spheres was measured. Then, the tube was then filled with a certain amount of deionized water, allowed to swell for 2 hours at room temperature, and the weight of the swollen spheres was measured. The following equation was used to calculate the swelling rate of the material.

$$\text{Swelling ratio \%} = [(Ws - W_0) / W_0] \times 100 \quad (3.1)$$

Where, W_0 and Ws are the weights of spheres before and after swelling, respectively.

The polymerization efficiency is calculated by dividing the dry weight of the polymer by the total amount of monomer used for the polymerization reaction. The polymerization yield of Stg-MIPs and NIPs was determined as percent polymerization yield. For this purpose, the dry weight of the synthesized polymers was weighed using a balance and the polymerization efficiency was calculated using the following equation:

$$\text{Polymerization Yield (\%)} = (m_{dry}/m_T) \times 100 \quad (3.2)$$

Here, m_{dry} represents the dry weight of the oven-dried polymer and m_T represents the total mass of monomers in the polymer mixture.

3.4.2. Fourier Transform Infrared Spectroscopy (FTIR)

Stg-MIPs and NIPs were characterized by FTIR (Jasco, FT/IR-6700, USA). For FTIR analysis, the synthesized Stg-MIPs and NIPs were placed in the device in powder form. N_2 gas was introduced into the sample chamber for 10 minutes to minimize interference from environmental gases and vapours on the sample spectrum. The spectrum was measured in the wavenumber range of 4000-400 cm^{-1}.

3.4.3. Surface Morphology

The morphological structures and particle sizes of Stg-MIPs and NIPs were investigated using scanning electron microscopy (SEM). Before SEM analysis, the Stg-MIPs and NIPs samples were swollen in deionized water and then dried in a lyophilizer (Lyophilizer, BK-FD10P, Biobase, China). The polymer samples taken after drying were fixed on the SEM sample plate using a conductive adhesive to take SEM images. The sample surface was coated with gold under vacuum, making the surface conductive, and SEM images of the polymers were taken at various magnifications.

3.5. Adsorption Studies

Adsorption-desorption kinetics are crucial in many circumstances where there are binding interactions. Stg adsorption of Stg-MIPs prepared at different concentrations was investigated in a batch system. For this purpose, 200 mg of the Stg-MIP and NIP polymers were weighed and conditioned with ethanol. Afterwards, different concentrations of Stg solutions (0.1,0.3,0.5,1,2,3,5,10 mg/mL) were prepared in ethanol. First, the initial absorbance values of the prepared solutions were measured at 205 nm using a UV spectrophotometer. After that Stg-MIPs and NIPs were interacted with different concentrations of Stg solutions (V=5 mL) for 2 hours. After 2 hours, final measurements were made at 205 nm to determine the amount of Stg adsorbed. Thus, the decrease in absorbance after adsorption was measured spectrophotometrically according to the initial absorbance value. Also temperature (4°C-40°C, 2 h) and interaction time (0-120 min.) on adsorption rate and capacity were investigated. The

Stg concentration determined (0.5 mg/mL) after the adsorption studies was used in the different temperatures and interaction times. Before these processes, the initial absorbance value of the selected Stg concentration (0.5 mg/mL) at 205 nm was measured. The determined Stg concentration (0.5 mg/mL, V=5 mL) was interacted with the polymer at 4, 25 and 40 °C for 2 hours. After 2 hours, absorbance measurements were taken. In different interaction times, polymers were exposed to Stg solution (0.5 mg/mL, V=5 mL) for 2 hours and samples were taken between 0 and 120 minutes and absorbance was measured. After each adsorption process for concentration, temperature and time scanning, the polymers were washed with ethanol. Also, polymers were incubated with methanol/acetic acid (9/1, v/v) for desorption studies.

The amount of Stg was calculated by creating a calibration curve with the adsorption amount of the solutions of Stg prepared between 0.1-10 mg/mL. A UV spectrophotometer at 205 nm was used and the adsorption capacity was calculated according to the following formula.

$$Q= [(C_0-C)\ xV] / m \quad (3.3)$$

Here, Q is the adsorption capacity (mg/g); C_0 and C are the concentrations of the Stg in the initial solutions and after process for a particular amount of time, respectively (mg/mL); V is the solution's volume (L) m is the mass of Stg used (g). For statistical calculations and quality control, each experiment was run multiple times.

3.6. Selectivity Studies

To define specificity of Stg-MIPs, a selectivity experiment as compared to competitor molecules was performed (Cholesterol (Chol, MW: 386.65 g/mol); Ergosterol (Erg, MW: 396.65 g/mol)). In the selectivity studies, solutions of Stg and competitor molecules (Cholesterol and Ergosterol) were prepared in ethanol (0.5 mg/mL) and initial absorbance measurements were made at 205 nm wavelength. Then, the solutions (V= 5 mL) interacted with polymers for 2 hours. At the end of 2 hours, final absorbances were measured. After each adsorption process, the polymers were washed with ethanol for 30 minutes and after washing, desorption was performed using methanol/acetic acid (9/1, v/v) solution. The absorbance of the samples taken after each treatment was measured at 205 nm.

The following equation was used to compute the distribution and selectivity coefficients of cholesterol and ergosterol with regard to Stg:

$$Q_d = [(C_i - C_f) / C_f] \times V/m \quad (3.4)$$

Here, Q_d stands in for the distribution coefficient; C_i and C_f are the initial and final concentrations of Stg, respectively. V is the solution's volume (mL) and m is the mass of the polymers used (g).

To evaluate the selective adsorption property of Stg-MIPs, the imprinting factor (IF) was calculated for Stg and competitors using the following equation:

$$IF = Qd_{Stg\text{-}MIP} / Qd_{NIP} \quad (3.5)$$

$Qd_{Stg\text{-}MIP}$ and Qd_{NIP} represent the distribution coefficients of Stg-MIPs and NIPs, respectively.

The equilibrium binding data were used to derive the selectivity coefficient for Stg binding in the presence of competing molecules using the following equation:

$$k = Q_d\,(\text{template}) / Q_d\,(\text{competitor}) \quad (3.6)$$

Competitors include substances such as Cholesterol and Ergosterol, and k is the selectivity coefficient. An assessment of the impact of imprinting on selectivity can be made by comparing the k values of the MIPs with those of the steroid molecules.

The relative selectivity coefficient k' (3.7) can be defined as:

$$k' = k_{imprinted} / k_{control} \quad (3.7)$$

3.7. Desorption and Reusability Studies

The desorption of Stg was carried out using a methanol/acetic acid (9/1, v/v) solution. After the adsorption studies, the polymers were treated with the desorption solution (V=5 mL) for 2 hours. Using a UV spectrophotometer, desorbed Stg from polymers was detected at 205 nm. After each desorption process, the polymers were washed with ethanol and prepared for their next use.

The desorption rate was deterined as follows according to the amount of Stg adsorbed by the polymers and the final Stg concentration in the medium as a result of desorption:

$$Desorption\ Ratio(\%) = \frac{amount\ of\ the\ desorpted\ stigmasterol}{amount\ of\ the\ adsorbed\ stigmasterol} x\ 100 \quad (3.8)$$

3.8. Stigmasterol from plant extract

Stg extraction from soybean oil was performed using the method reported by Sinha et al., 2015. First, 5 mL of ethanolic KOH (0.5 M) solution was added to 4 mL of soybean oil and mixed for 15 minutes. The mixture was heated in a water bath at 80 ºC for 30 minutes and then cooled to room temperature. Next, 3 mL of hexane and 2 mL of distilled water were added to the mixture and it was allowed to mix for 15 minutes. After mixing, the sample was centrifuged at 3000 rpm to observe the phase separation and collect the hexane fraction containing Stg. The hexane was evaporated using a BUCHI brand evaporator (Rotavapor R-300, Switzerland). The residue was dissolved in 2 mL ethanol. For adsorption, 5 mL of soybean oil is mixed with 200 mg Stg-MIP and NIP. Then, 0.1 and 3 mg/mL Stg concentrations were added to the sample and stirred for 2 hours. After adsorption studies; the absorbances of the initial, final and desorption solutions were measured spectrophotometrically.

4. RESULTS AND DISCUSSIONS

4.1. Characterization of Stg-MIPs and NIPs

4.1.1. Swelling Test and Polymerization Yield

Swelling experiments were used to determine the swelling ratio and polymerization yield. The percentages of swelling and polymerization yield for Stg-MIPs and NIPs were calculated as shown in Table 4.1. When the results were evaluated, it was observed that the swelling percentages of Stg-MIP polymers were lower compared to NIPs. The inclusion of the Stg-VBA pre-complex in the structure increased the hydrophobic property of the polymer, and accordingly, it was determined that the swelling percentages of Stg-MIP polymers were lower

compared to NIPs. In addition, the lower swelling rate and polymerization yield of MIPs than NIPs may be due to material loss from repeated template removal processes.

Table 4. 2. Swelling ratio and polymerization yield of Stg-MIPs and NIPs.

Polymers	Swelling Rate, %	Polymerization Yield, %
Stg-MIPs	113,5	89,7
NIPs	146,3	98,2

4.1.2. SEM Studies

The surface morphology of the polymers (Stg-MIPs and NIPs) was investigated by SEM at different magnifications (20.000X and 5.000X). SEM images of Stg-MIPs and NIPs are given in Figure 4.1. SEM photographs were examined and the average diameter of the polymers selected from the images was calculated as 1 μm with the Image J program. It has been observed that both polymers have a monosize structure. The small and monosize structure of the polymers provides fast adsorption kinetics and reproducible results. Obtained experimental results supported this prediction.

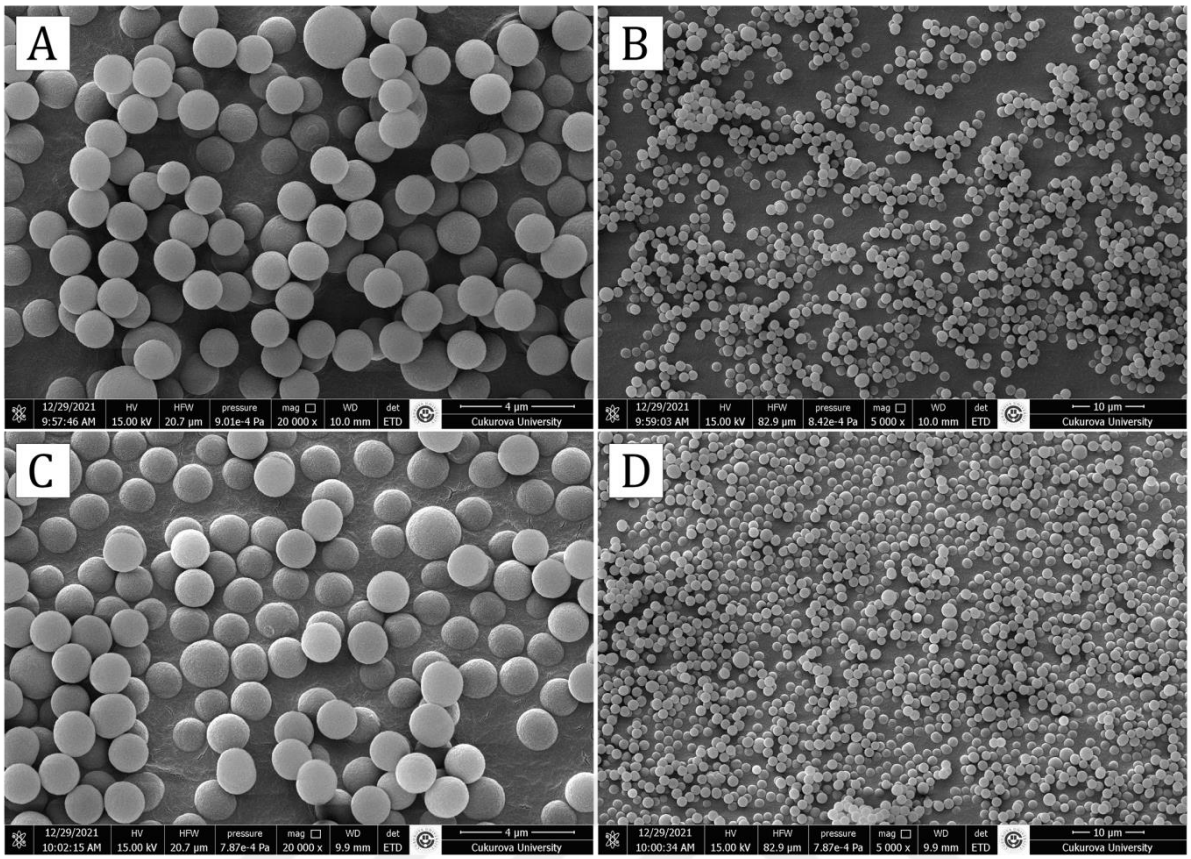

Figure 4. 1. SEM Analysis. SEM images of A) Stg-MIPs (20.000 x), B) Stg-MIPs (5000 x), C) NIPs (20.000 x), D) NIPs (5000 x).

4.1.3. FTIR Studies

The characterization of the chemical structures of the synthesized polymers was done by Fourier transform infrared spectroscopy (FTIR). The spectrum obtained for Stg-MIPs and NIPs are shown in Figure 4.2.

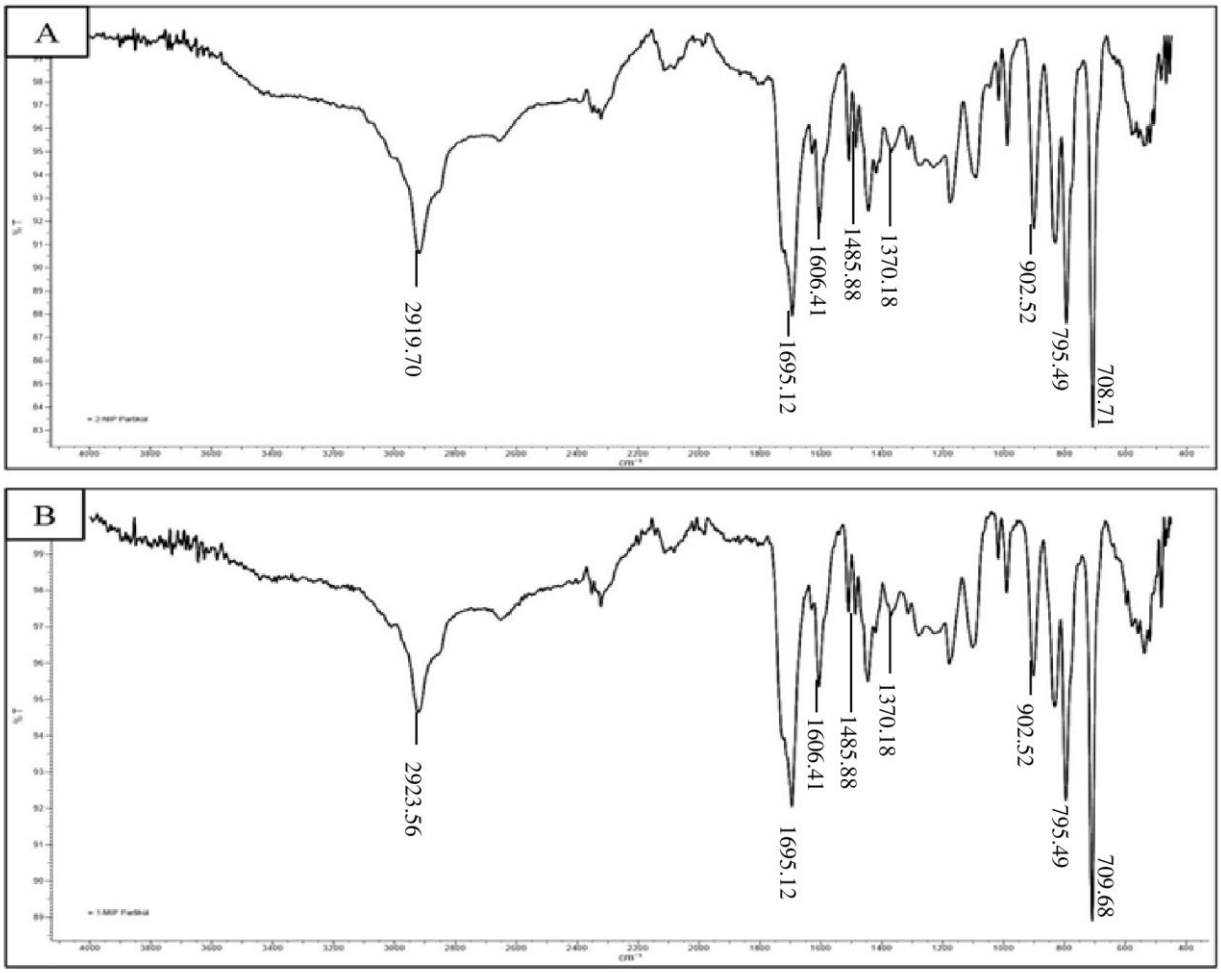

Figure 4. 2. FTIR Analysis. FTIR images of A) NIPs, B) Stg-MIPs.

Figure 4.2. shows the FTIR spectra of Stg-MIP and NIP polymers. Because the structures of Stg-MIP and NIP polymers are so similar, their spectra are as well. Despite the fact that the structure's intense MAA and DVB-80 content screens the VBA and Stg molecules that enter it, the presence of these molecules has been successfully demonstrated. The peaks seen around 1695.12 cm^{-1}, 1606.41 cm^{-1}, 1485.88 cm^{-1}, and 1370.18 cm^{-1} in DVB-80 are associated with the benzene ring structure, which is common in their structure. The C-H tensile bands in MAA and DVB-80 content cause peaks around 795.49 cm^{-1} and 902.52 cm^{-1}. These peaks are seen in both spectra as common bands.

In NIP, the frequency of vibrational movements of O-H groups was around 2919.70 cm^{-1}, but in Stg-MIP, it shifted to 2923.56 cm^{-1} (higher frequency). This demonstrates that VBA is embedded in the structure of Stg-MIP polymers. In addition, the frequency of aromatic and aliphatic double bond vibrational movements shifted from 708.71 cm^{-1} to 709.68 cm^{-1}. These spectral changes indicate the presence of the Stg-VBA pre-complex molecule in the structure.

4.2. Adsorption Studies

Adsorption and desorption studies were performed with Stg solutions prepared at various concentrations to determine the optimum conditions for adsorption of Stg-MIPs and NIPs. The effects of initial Stg concentration, temperature, and interaction time on Stg-MIPs adsorption capacity were studied. In addition, Ergosterol and Cholesterol competitor molecules which are similar chemical structure to Stg were used to demonstrate the selectivity of Stg-MIPs. To examine the reusability of the Stg-MIPs, ten times the adsorption and desorption experiments were carried out using the same polymer under the same conditions. Obtained results are given in detail in this section.

4.2.1. The Effect of Initial Stigmasterol Concentration

Stg solutions were prepared at various concentrations (0.1, 0.3, 0.5, 1, 2, 3, 5, 10 mg/mL) in ethanol to assess the impact of starting concentrations on adsorption capacity. Then, 200 mg of Stg-MIPs and NIPs were weighed. Stg solutions prepared at different concentrations were added to each weighted polymer (v=5 mL) and polymers and solutions were interacted for 2 hours at 25 ℃. The results of the study with Stg-MIPs and NIPs are given in Figure 4.3. Almost all concentrations of Stg molecules were adsorbed by the imprinted polymers. Although the maximum adsorption capacity of Stg-MIPs did not change, the concentration of Stg continued to rise after 3 mg/mL due to binding site saturation. The maximum Stg adsorption capacity of Stg-MIPs was determined as 73.2 mg/g. It was observed that the Stg binding capacity of NIPs was very low compared to MIPs. The highest binding capacity for NIPs was determined as 8 mg/g.

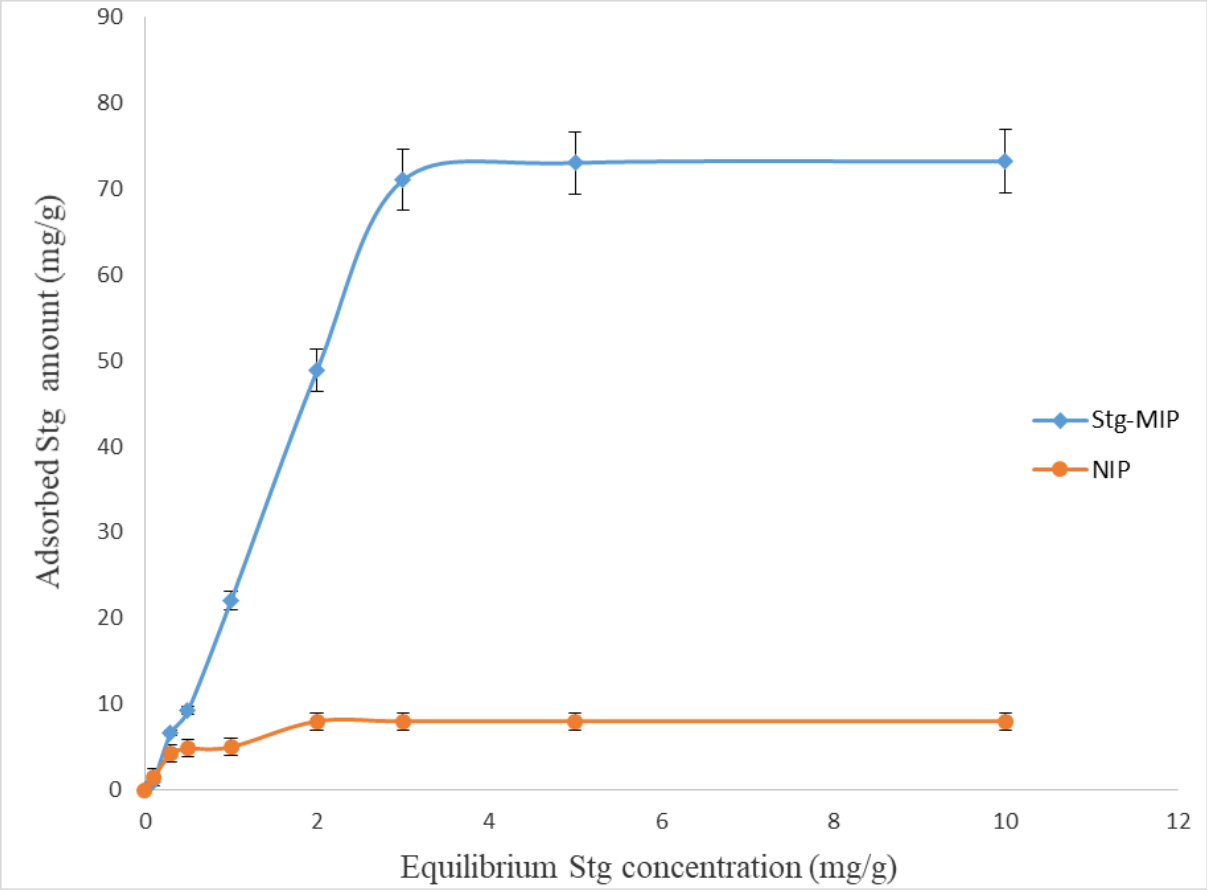

Figure 4. 3. Effect of the initial Stg concentration on Stg adsorption (0,1-10 mg/mL Stg in ethanol, T: 25°C, V: 5 mL, time: 2 h).

4.2.2. Adsorption Isotherms

Adsorption isotherms are used to explain the interaction between any molecule and its adsorbent. These isotherms show the relationship between the concentration of molecules adsorbed on the solid phase and the concentration of molecules in the solution when the two phases are in equilibrium. In this study, Langmuir and Freundlich adsorption isotherm models were used to characterize the interaction of Stg-MIP and Stg molecules in solution medium. According to the Langmuir adsorption model, monolayer adsorption takes place. Adsorption occurs only in a few discrete, quivalent regions, and there is no lateral interaction or steric

inhibiton between adsorbed molecules, even in adjacent regions (Foo and Hameed, 2010). The Langmuir adsorption isotherm is expressed using the following formula:

$$Q_e = Q_{max} \cdot b \cdot C_e / (1 + b \cdot C_e) \quad (4.1)$$

This equation can be linearized as follows:

$$C_e/ Q_e = 1 / (Q_{max} \cdot b) + (C_e / Q_{max}) \quad (4.2)$$

Where, Q_e represents the concentration of Stg adsorbed to the adsorbent. Q_{max} is the maximum adsorption capacity of Stg (mg/g) and b is the Langmuir constant (mL/mg). C_e is the equilibrium concentration of Stg in solution (mg/mL). It is possible to determine the Q_{max} and b values by plotting the C_e/ Q_e versus C_e graph (Figure 4.4a).

In contrast to the Langmuir adsorption isotherm model, the Freundlich adsorption isotherm model explains why the adsorption surface has a heterogeneous surface energy. Active binding sites that are close to each other, according to this model, interact with each other.

The equation for the Freundlich adsorption isotherm is as follows:

$$Q_e = Q_f \cdot (C_e)^{1/n} \quad (4.3)$$

Here, Q_f (mg/g) is the maximum Stg adsorption capacity according to the Freundlich adsorption model. The Freundlich constant, which characterizes the system's heterogeneity, is 1/n. The above equation can be made linear as follows by taking the logarithm of both sides.

$$\ln Q_e = \ln Q_f + 1/n \cdot \ln C_e \quad (4.4)$$

Q_f and 1/n can be determined by plotting $\ln Q_e$ versus $\ln C_e$ (Figure 4.4 b).

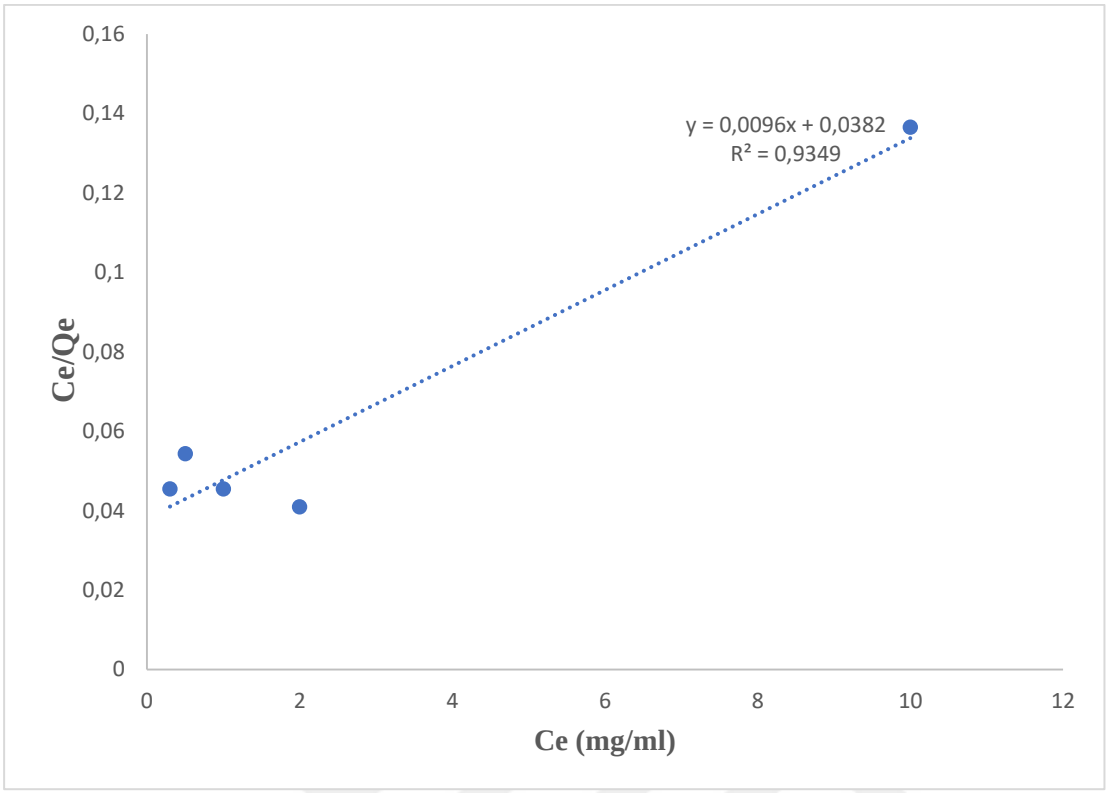

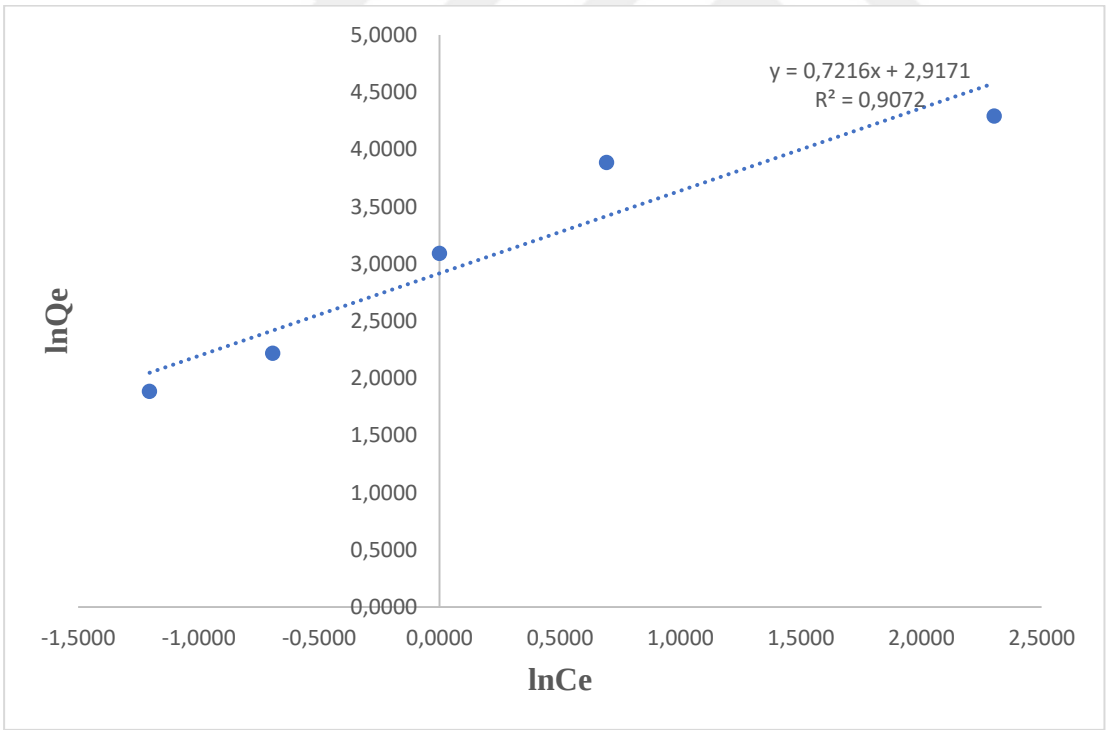

Figure 4. 4. a) Langmuir adsorption isotherm model b) Freundlich adsorption isotherm model.

The correlation coefficient of the Langmuir isotherm model (R^2= 0.93), was found to be higher than the correlation coefficient of the Freundlich isotherm model (R^2= 0.90). The high correlation coefficient (R^2) value obtained from the Langmuir isotherm shows that the system is suitable for the Langmuir adsorption model and that the Stg molecules are placed on the synthesized polymers in a monosized layer. It also shows that the polymer surface is homogeneous in terms of adsorption areas and energy. Maximum adsorption amounts of Langmuir and Freundlich adsorption models were calculated and these values were determined as 104.16 and 18.48 mg/g, respectively. The results showed that the maximum adsorption amount of Langmuir adsorption models was closer to the maximum adsorption amount obtained in experimental studies (73.2 mg/g) than that of the Freundlich adsorption model. The adsorption constants b and n of both models were found to be 0.25 and 1.38, respectively (Table 4.2).

Table 4. 3. The isotherm constants for Langmuir and Freundlich adsorption.

Experimental	Langmuir			Freundlich		
Q_e (mg/g)	Q_{max} (mg/g)	b (mL/mg)	R^2	Q_f (mg/g)	N	R^2
73.2	104.16	0.25	0.93	18.48	1.38	0.90

4.2.3. The Effect of Interaction Time on Stigmasterol Adsorption

Stg-MIPs were interacted with Stg for 2 hours. Samples were taken at different time periods and their measurements were carried out. As seen in Figure 4.4, an increase in Stg adsorption was observed until the 60th minute. There was minimal difference in the amount of adsorption after 60th minutes.

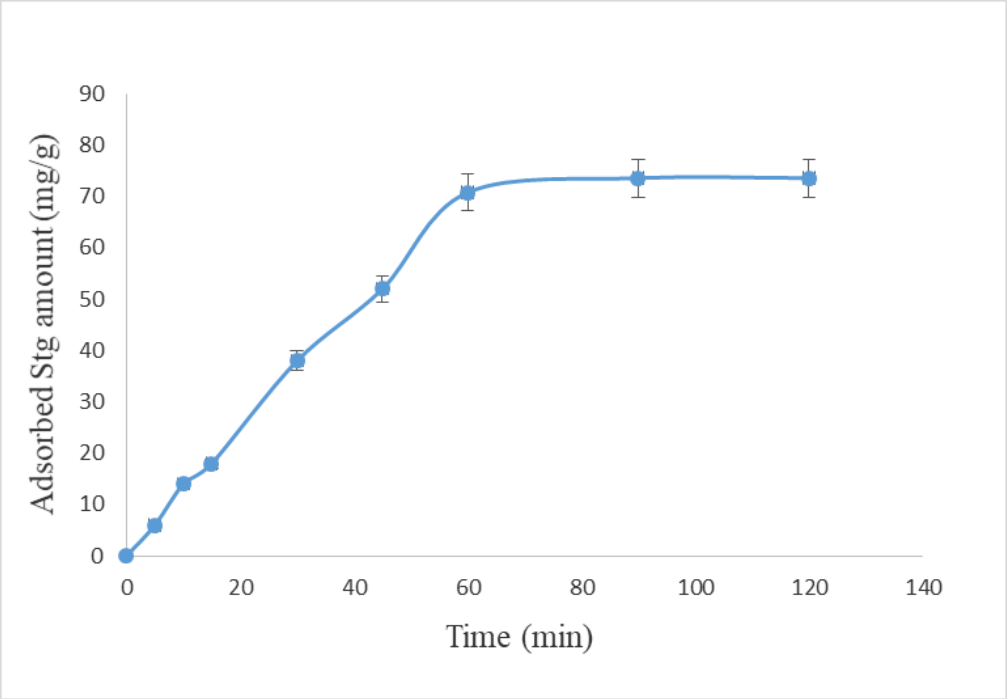

Figure 4. 5. Effect of interaction time on Stg adsorption (Initial Stg concentration: 0-120 min., 0.5 mg/mL, T: 25°C, V: 5 mL).

Adsorption kinetic models can be used to investigate the adsorption process's control mechanisms, such as mass transfer and chemical reactions. The experimental data show that the Stg concentration on the adsorbent surface and the Stg concentration in the solution are equal. Lagergren's first-order rate equation is one of the most commonly used equations for solute absorption from a liquid solution.

$$dq_t / d_t = k_1.(q_{eq}-q_t) \quad (4.5)$$

The pseudo-first order adsorption rate constant, or k1, is 1/min. The amount of Stg adsorbed at equilibrium is called qeq (mg/g) and the amount of Stg adsorbed at time t is called qt (mg/g). At t = 0, at the time $q_t = 0$ and t = t, the following equation is obtained as a result of applying and integrating the boundary conditions qt = qt:

$$\log[q_{eq} / (q_{eq} - q_t)] = (k_1.t) / 2.303 \quad (4.6)$$

The equation can be linearized in the following way:

$$\log(q_{eq} - q_t) = \log (q_{eq}) - (k_1.t) / 2.303 \quad (4.7)$$

The linearity of the log(qeq) versus t plot demonstrates the kinetic model's applicability. The pseudo-second order equation based on the adsorption equilibrium capacity is given below:

$$dq_t / d_t = k_2.(q_{eq} - q_t)^2 \quad (4.8)$$

k_2 is the pseudo-second order rate constant ($g.mg^{-1}.min^{-1}$). The equation is linearized to get the following equation:

$$(t / q_t) = (1 / k_2.q_{eq}^{\ 2}) + (1 / q_{eq}). t \quad (4.9)$$

The plot of t/qt versus t must be linear for second-order kinetics to be applicable. The rate constant (k_2) can be determined from the cutoff point, the equilibrium adsorption (q_{eq}) from the slope.

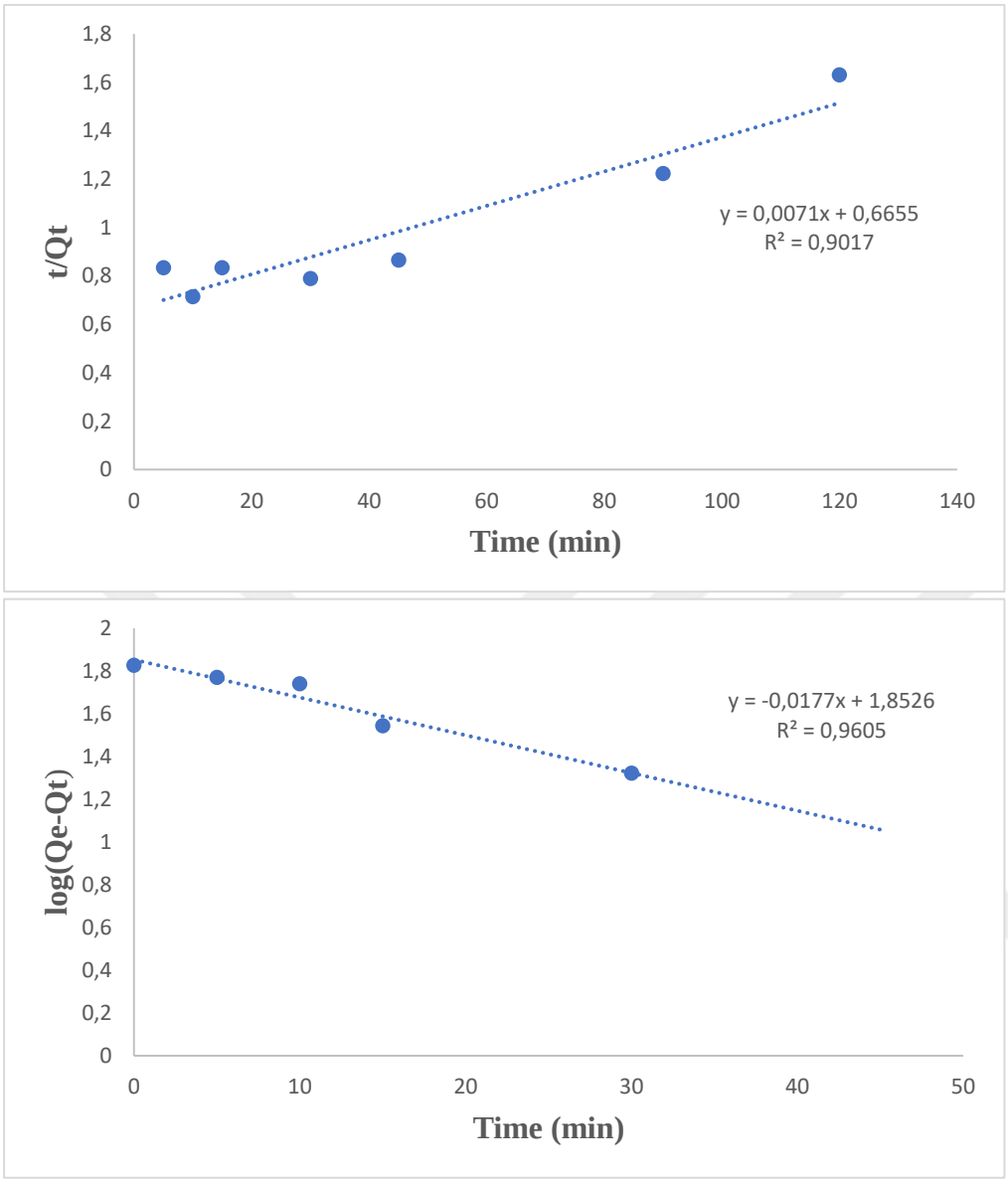

Figure 4. 6. The graph of a) Pseudo first order kinetic model b) Pseudo second order kinetic model

First and second order kinetic calculations of Stg adsorption by Stg-MIPs are given in Table 4.3. When the results are compared, it is seen that the correlation coefficient (R^2=0,96) of the second-order kinetic model is higher. The findings show that this experimental system can be explained with a second-order kinetic model. Therefore, the diffusion limits of Stg adsorption by Stg-MIP are negligible. The kinetic behavior is controlled by the spesific binding reaction between Stg-MIPs and Stg molecules.

Table 4. 4. Adsorption kinetic model constants.

Initial concentration (mg/ml)	Experimental	Pseudo first order kinetic			Pseudo second order kinetic		
	Qe (mg/g)	k1 (1/dk)	Qe (mg/g)	R^2	k2 (1/dk)	Qe (mg/g)	R^2
	73.2 mg/g	-0.01	1.95	0.90	0.0005	-56.5	0.96

4.2.4. The Effect of Temperature on Stigmasterol Adsorption

The effect of temperature on Stg adsorption was determined by performing adsorption studies with Stg-MIPs at 4, 25 and 40 ℃. As seen in Figure 4.5, the adsorption capacities of Stg-MIPs decreased with increasing temperature. The highest adsorption capacity of Stg-MIPs (93.6 mg/g) was determined at 4 ℃. Secondary interactions such as electrostatic interactions, dipole-dipole interactions, and hydrogen bonds weaken as temperature rises. According to studies, the adsorption capacity formed by hydrophobic interactions decreases with increasing temperature, implying that the interaction between Stg-MIPs and Stg occurs via secondary interactions. Furthermore, physical adsorption is an exothermic process, therefore it happens more readily at lower temperatures and becomes less effective as the temperature rises. Physical adsorption may have contributed to the reduction in Stg adsorption capacity.

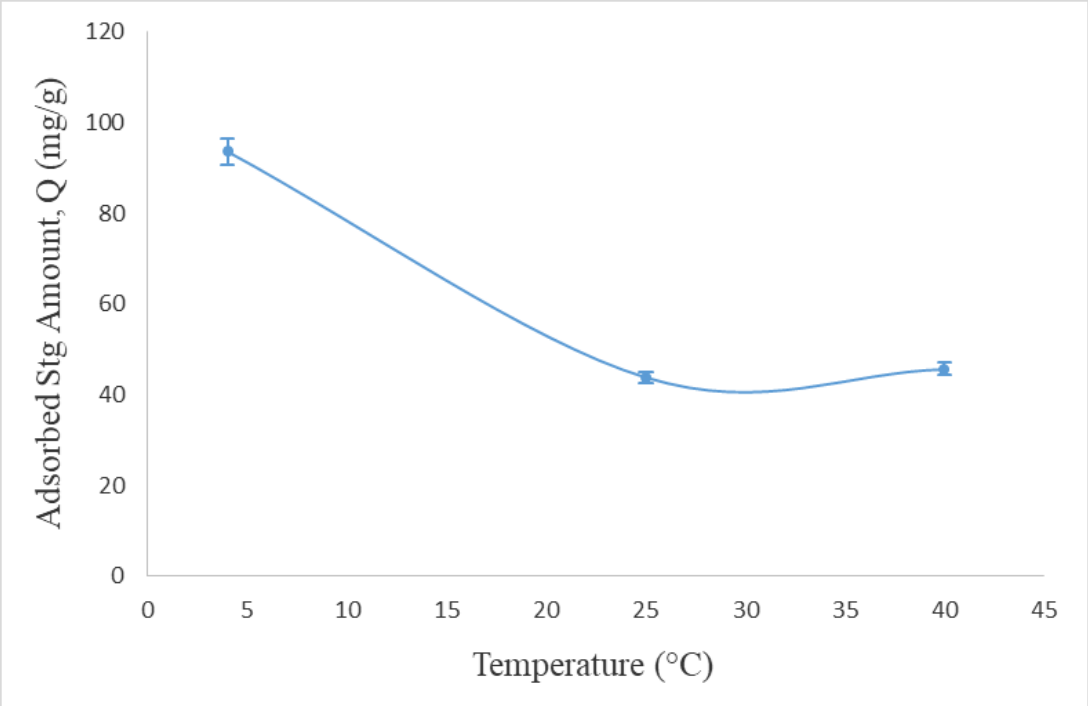

Figure 4. 7. Effect of temperature on Stg adsorption (Initial Stg concentration: 0.5 mg/mL, V: 5 mL, time: 2 h).

4.3. Selectivity Studies

The selectivity of synthesized Stg-MIPs against Stg was investigated using Ergosterol and Cholesterol competitor molecules. These two molecules were chosen as competitor molecules because their chemical structures are similar to Stg. The chemical structures of Stg and competitor molecules are shown in Figure 4.6.

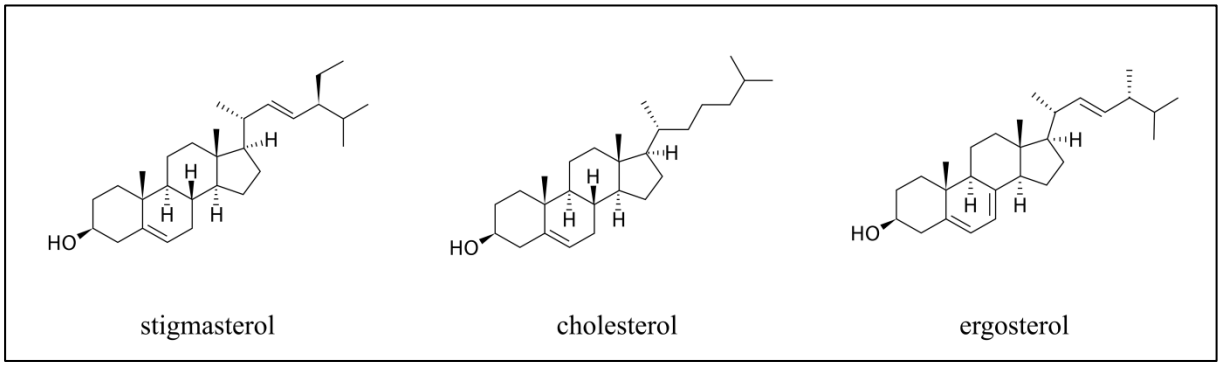

Figure 4. 8. Chemical Structure of Stg, Cholesterol and Ergosterol.

First, Ergosterol and Cholesterol molecules were dissolved in ethanol to prepare at the specified concentration (0.5 mg/mL). The prepared solutions interacted with 200 mg of Stg-MIPs and NIPs for 2 h at 25 ℃. Samples taken at the end of the process were measured spectrophotometrically at 205 nm. The concentrations of absorbed molecules by Stg-MIPs were found to be 12.69 mg/g, 8.75 mg/g and 4.64 mg/g for Stg, Chol and Erg, respectively. Also the concentrations of absorbed molecules by NIPs were determined as 4.58 mg/g, 12.47 mg/g and 22.94 mg/g for Stg, Chol and Erg. According to the results of the selectivity studies, the Stg adsorption amounts of Stg-MIPs were quite high compared to competitors and NIPs (Figure 4.7). In this regard, the Qd, k and IF values of Stg-MIPs and NIPs were calculated using the equations given in section 3.6. The results are given in Table 4.4.

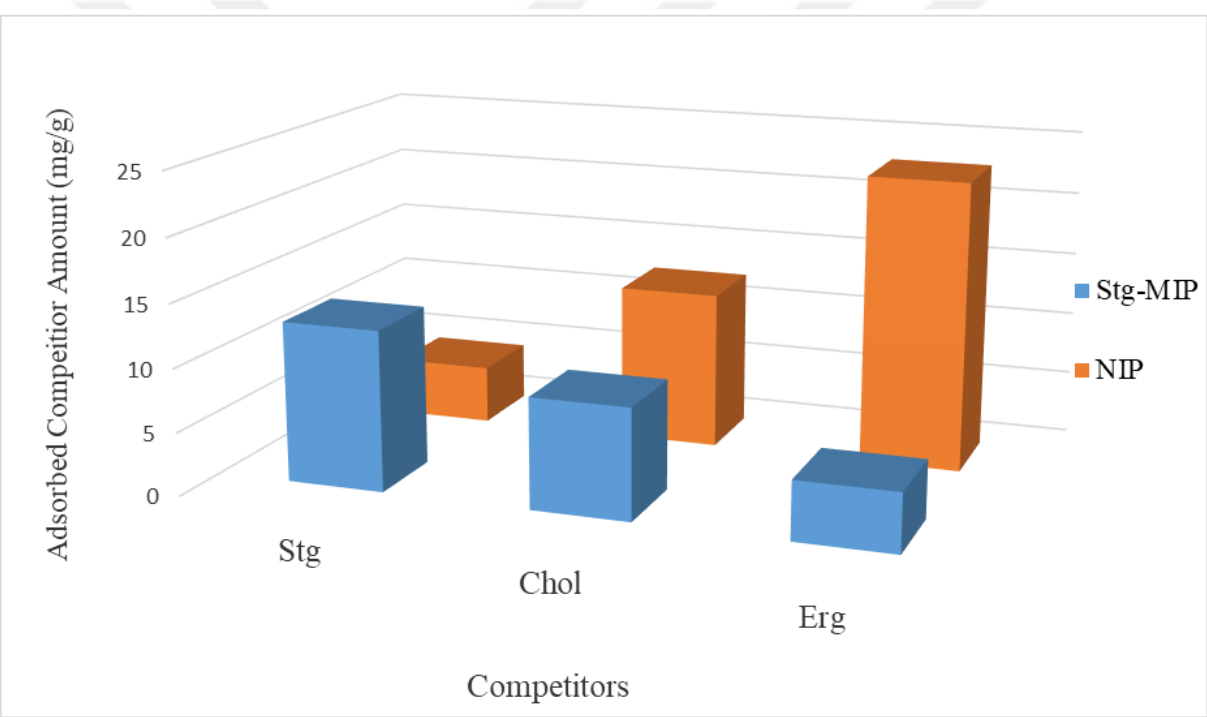

Figure 4. 9. Selectivity studies (Ergosterol and Cholesterol).

Table 4. 5. Selective adsorption properties of Stg-MIPs in the presence of competitors.

	QdMIP (mg/g)	QdNIP (mg/g)	IF	kMIP	kNIP	k'
Stg	12.69	4.58	2.77	1	1	1
Chol	8.75	12.47	0.7	1.45	0.36	3.95
Erg	4.64	22.94	0.2	2.73	0.2	13.69

4.4. Desorption and Reusability Studies

Stg-MIPs interacted with the same concentration of Stg solution 10 times in a row to determine the reusability. The amounts of adsorbed and desorbed Stg in each cycle were recorded and the results are shown in Figure 4.8. It was determined that the Stg adsorption capacity of the polymers decreased from 73.2 mg/g to 70.2 mg/g at the end of the 10th cycle. The Stg-MIP adsorption capacity was reported to be nearly 96%. There was no significant decrease in the adsorption capacity of Stg-MIPs after 10 repetitions.

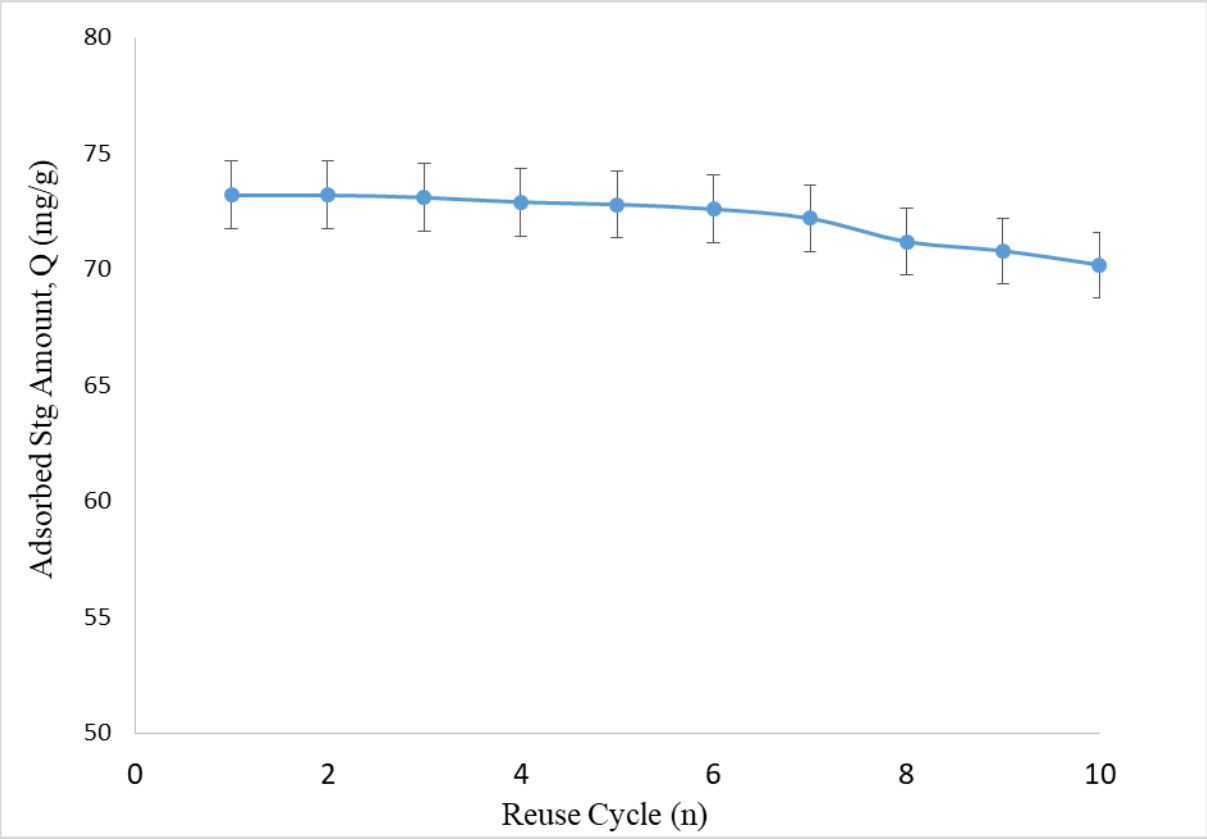

Figure 4. 10. Reusability of Stg-MIPs (Stg concentration: 0,5 mg/mL, V: 5 mL, time: 2 h).

4.5. Stigmasterol Extraction From Plant Extract

In order to determine the Stg adsorption capacity of Stg-MIPs from soybean oil extract, different concentrations of Stg were added into the soybean oil extract. The initial absorbance values of these prepared concentrations were measured spectrophotometrically. Concentrations were interacted with Stg-MIP polymers for 2 hours and absorbance measurements of the final samples were taken after 2 hours. After the adsorption process was finished, desorption was done for 30 minutes and the absorbance of the desorption samples was measured in a similar way. The results are given in Table 4.5.

Table 4. 6. Stg extraction from soybean oil extract.

Sample	Added Stg amount (mg/mL)	Recovery (%)	Relative standard deviation (%)
Extract from Soybean Oil	0,1	82.72	1.68
	3	84.65	1.90

Recovery (%) = (measurement of sample with added Stg- measurement of sample of soybean oil / concentration of Stg added at baseline) x 100

Relative standard deviation (%) = (standard deviation/mean) x 100

5. CONCLUSION

In this thesis, Stg-imprinted solid phase extraction polymer was developed for direct determination of Stg from plant extract with a brand new method. Thus, a highly selective, specific and effective method has been developed for the direct analysis of Stg, which is one of the phytosterols naturally found in plant and has many positive effect on human health. The swelling ratios of NIPs and Stg-MIPs polymers used in this study were found to be 146.3 and 113.5, respectively. Characterization studies of the synthesized polymers were carried out by SEM, FTIR and swelling tests. The surface morphology of Stg-MIPs and NIPs has been studied and shown that the both polymers have a monosize structure by SEM photographs. Adsorption properties, selectivity for Stg and reusability were tested by kinetic studies. In adsorption studies, the effects of initial Stg concentration, interaction time and temperature on Stg adsorption were analyzed separately. According to the results of the selectivity studies, the Stg adsorption amounts of Stg-MIPs were found to be quite high compared to competitor Ergosterol and Cholesterol molecules and NIPs. Adsorption-desorption studies show that Stg-MIP retains

its selective Stg adsorption capacity without significant reduction even in the tenth cycle. Also, adsorption studies were carried out with stigmasterol extracted from soybean oil and around 80% recovery was obtained at different concentrations. In the light of all these studies, Stg imprinted solid phase extraction polymers can be used as an alternative method for the determination of Stg. It is seen that it has commercialization potential due to its high selectivity and reusability.

REFERENCES

Afroz, M., Zihad, S. M. N. K., Uddin, S. J., Rouf, R., Rahman, Md. S., Islam, M. T., … Sarker, S. D. (2019). A systematic review on antioxidant and antiinflammatory activity of Sesame Sesamum indicum oil and further confirmation of antiinflammatory activity by chemical profiling and molecular docking. *Phytotherapy Research*, *33*(10), 2585–2608.

Ahmad Khan, M., Sarwar, A. H. Md. G., Rahat, R., Ahmed, R. S., & Umar, S. (2020). Stigmasterol protects rats from collagen induced arthritis by inhibiting proinflammatory cytokines. International Immunopharmacology, 85, 106642.

al Shannaq, R., & Farid, M. M. (2015). Microencapsulation of phase change materials (PCMs) for thermal energy storage systems. Advances in Thermal Energy Storage Systems: Methods and Applications, 247–284.

Alexander, C., Andersson, H. S., Andersson, L. I., Ansell, R. J., Kirsch, N., Nicholls, I. A., … Whitcombe, M. J. (2006, March). Molecular imprinting science and technology: A survey of the literature for the years up to and including 2003. Journal of Molecular Recognition.

Ali, H., Dixit, S., Ali, D., Alqahtani, S. M., Alkahtani, S., & Alarifi, S. (2015). Isolation and evaluation of anticancer efficacy of stigmasterol in a mouse model of DMBA-induced skin carcinoma. Drug Design, Development and Therapy, 9, 2793–2800.

Alizadeh, T., & Memarbashi, N. (2012). Evaluation of the facilitated transport capabilities of nano- and micro-sized molecularly imprinted polymers (MIPs) in a bulk liquid membrane system. Separation and Purification Technology, 90, 83–91.

Antwi, A. O., Obiri, D. D., & Osafo, N. (2017). Stigmasterol Modulates Allergic Airway Inflammation in Guinea Pig Model of Ovalbumin-Induced Asthma. Mediators of Inflammation, 2017.

Barriuso, B., Ansorena, D., Poyato, C., & Astiasarán, I. (2015). Cholesterol and stigmasterol within a sunflower oil matrix: Thermal degradation and oxysterols formation. Steroids, 99, 155–160.

Batta, A. K., Xu, G., Honda, A., Miyazaki, T., & Salen, G. (2006). Stigmasterol reduces plasma cholesterol levels and inhibits hepatic synthesis and intestinal absorption in the rat. Metabolism, 55(3), 292–299.

Bayram, E., Yılmaz, E., Uzun, L., Say, R., & Denizli, A. (2017). Multiclonal plastic antibodies for selective aflatoxin extraction from food samples. Food Chemistry, 221, 829–837.

Bereli, N., Akgönüllü, S., Aslıyüce, S., Çimen, D., Göktürk, İ., Türkmen, D., Denizli, A. (2020). Molecular Imprinting Technology for Biomimetic Assemblies. Hacettepe Journal of Biology and Chemistry.

Carter, B. A., Taylor, O. A., Prendergast, D. R., Zimmerman, T. L., von Furstenberg, R., Moore, D. D., & Karpen, S. J. (2007). Stigmasterol, a Soy Lipid–Derived Phytosterol, Is an Antagonist of the Bile Acid Nuclear Receptor FXR. Pediatric Research, 62(3), 301–306.

Cela-Pérez, M. C., Lasagabáster-Latorre, A., Abad-López, M. J., López-Vilariño, J. M., & Gónzalez-Rodríguez, M. v. (2013). A study of competitive molecular interaction effects on imprinting of molecularly imprinted polymers. Vibrational Spectroscopy, 65, 74–83.

Cunningham, V. J., Alswieleh, A. M., Thompson, K. L., Williams, M., Leggett, G. J., Armes, S. P., & Musa, O. M. (2014). Poly(glycerol monomethacrylate)-poly(benzyl methacrylate) diblock copolymer nanoparticles via RAFT emulsion polymerization: Synthesis, characterization, and interfacial activity. Macromolecules, 47(16), 5613–5623.

De-Eknamkul, W., & Potduang, B. (2003). Biosynthesis of β-sitosterol and stigmasterol in Croton sublyratus proceeds via a mixed origin of isoprene units. Phytochemistry, 62(3), 389–398.

Demirkurt, M., Olcer, Y. A., Demir, M. M., & Eroglu, A. E. (2018). Electrospun polystyrene fibers knitted around imprinted acrylate microspheres as sorbent for paraben derivatives. Analytica Chimica Acta, 1014, 1–9.

Fernandes, P., & Cabral, J. M. S. (2007). Phytosterols: Applications and recovery methods. Bioresource Technology, 98(12), 2335–2350.

Foo, K. Y., & Hameed, B. H. (2010). Insights into the modeling of adsorption isotherm systems. Chemical engineering journal, 156(1), 2-10.

Gabay, O., Sanchez, C., Salvat, C., Chevy, F., Breton, M., Nourissat, G., … Berenbaum, F. (2010). Stigmasterol: a phytosterol with potential anti-osteoarthritic properties. Osteoarthritis and Cartilage, 18(1), 106–116.

Garcia, R., Carreiro, E. P., Prates Ramalho, J. P., Mirão, J., Burke, A. J., Gomes da Silva, M. D. R., … Cabrita, M. J. (2018). A magnetic controllable tool for the selective enrichment of dimethoate from olive oil samples: A responsive molecular imprinting-based approach. Food Chemistry, 254, 309–316.

Giovannoli, C., Passini, C., Anfossi, L., di Nardo, F., Spano, G., Maurino, V., & Baggiani, C. (2015). Comparison of binding behavior for molecularly imprinted polymers prepared by hierarchical imprinting or Pickering emulsion polymerization. Journal of Separation Science, 38(20), 3661–3668.

Grandmougin-Ferjani, A., Schuler-Muller, I., & Hartmann, M. A. (1997). Sterol Modulation of the Plasma Membrane H+-ATPase Activity from Corn Roots Reconstituted into Soybean Lipids. Plant Physiology, 113(1), 163–174.

Gu, T., Hsu, K. H., & Syu, M. J. (2003). Scale-up of affinity chromatography for purification of enzymes and other proteins. Enzyme and Microbial Technology, 33(4), 430–437. doi:10.1016/S0141-0229(03)00141-8

Hage, D. S., Anguizola, J. A., Bi, C., Li, R., Matsuda, R., Papastavros, E., … Zheng, X. (2012). Pharmaceutical and biomedical applications of affinity chromatography: Recent trends and developments. Journal of Pharmaceutical and Biomedical Analysis, 69, 93–105.

Halhalli, M. R., & Sellergren, B. (2015a). Insights into the formation, structural properties and performance of RAFT polymerized L-phenylalanine anilide molecularly imprinted polymers. Polymer Chemistry, 6(41), 7320–7332.

Halhalli, M. R., & Sellergren, B. (2015b). Insights into the formation, structural properties and performance of RAFT polymerized L-phenylalanine anilide molecularly imprinted polymers. Polymer Chemistry, 6(41), 7320–7332.

Harborne, J. B. (Jeffrey B.). (1998). Phytochemical methods : a guide to modern techniques of plant analysis. Chapman and Hall.

Hartmann, M. (1998). Plant sterols and the membrane environment. Trends in Plant Science, 3(5), 170–175.

Hashim, S. N. N. S., Boysen, R. I., Schwarz, L. J., Danylec, B., & Hearn, M. T. W. (2014). A comparison of covalent and non-covalent imprinting strategies for the synthesis of stigmasterol imprinted polymers. Journal of Chromatography A, 1359, 35–43.

Hood, M. A., Mari, M., & Muñoz-Espí, R. (2014). Synthetic Strategies in the Preparation of Polymer/Inorganic Hybrid Nanoparticles. Materials 2014, Vol. 7, Pages 4057-4087, 7(5), 4057–4087.

Jayasinghe, G. D. T. M., & Moreda-Piñeiro, A. (2021). Molecularly Imprinted Polymers for Dispersive (Micro)Solid Phase Extraction: A Review. Separations, 8(7), 99.

Kamaruzaman, S., Nasir, N. M., Faudzi, S. M. M., Yahaya, N., Hanapi, N. S. M., & Ibrahim, W. N. W. (2021). Solid-Phase Extraction of Active Compounds from Natural Products by Molecularly Imprinted Polymers: Synthesis and Extraction Parameters. Polymers 2021, Vol. 13, Page 3780, 13(21), 3780.

Kangsamaksin, T., Chaithongyot, S., Wootthichairangsan, C., Hanchaina, R., Tangshewinsirikul, C., & Svasti, J. (2017). Lupeol and stigmasterol suppress tumor angiogenesis and inhibit cholangiocarcinoma growth in mice via downregulation of tumor necrosis factor-α. PloS One, 12(12).

Kaur, N., Chaudhary, J., Jain, A., & Kishore, L. (2011). STIGMASTEROL: A COMPREHENSIVE REVIEW. IJPSR, 2(9).

Kempe, M., & Mosbach, K. (1995). Molecular imprinting used for chiral separations. Journal of Chromatography A, 694(1), 3–13.

Koohpaei, A. R., Shahtaheri, S. J., Ganjali, M. R., Forushani, A. R., & Golbabaei, F. (2008). Application of multivariate analysis to the screening of molecularly imprinted polymers (MIPs) for ametryn. Talanta, 75(4), 978–986.

Krajewski-Bertrand, M.-A., Milon, A., & Hartmann, M.-A. (1992). Deuterium-NMR investigation of plant sterol effects on soybean phosphatidylcholine acyl chain ordering. Chemistry and Physics of Lipids, 63(3), 235–241.

Kumar, S., Kumar, V., & Prakash, O. (2013). Enzymes inhibition and antidiabetic effect of isolated constituents from Dillenia indica. BioMed Research International, 2013.

Lagarda, M. J., García-Llatas, G., & Farré, R. (2006). Analysis of phytosterols in foods. Journal of Pharmaceutical and Biomedical Analysis, 41(5), 1486–1496.

Lengyel, J., Rimarčík, J., Vagánek, A., Fedor, J., Lukeš, V., & Klein, E. (2012). Oxidation of sterols: Energetics of C–H and O–H bond cleavage. Food Chemistry, 133(4), 1435–1440.

Liang, Q., Yang, J., He, J., Chen, X., Zhang, H., Jia, M., … Wei, J. (2020). Stigmasterol alleviates cerebral ischemia/reperfusion injury by attenuating inflammation and improving antioxidant defenses in rats. Bioscience Reports, 40(4), 20192133.

Lindsey, K., Pullen, M. L., & Topping, J. F. (2003). Importance of plant sterols in pattern formation and hormone signalling. Trends in Plant Science, 8(11), 521–525.

Liška, I. (2000). Fifty years of solid-phase extraction in water analysis – historical development and overview. Journal of Chromatography A, 885(1–2), 3–16.

Lu, H., Tian, H., Wang, C., & Xu, S. (2020). Designing and controlling the morphology of spherical molecularly imprinted polymers. Materials Advances, 1(7), 2182–2201.

Marjanovic, M., Schranzhofer, L., Jungmann, C., -, al, Si, B., Song -, E., … Taba, P. (2020). Synthesis and characterization of stigmasterol imprinted polymers with precipitation polymerization method. IOP Conference Series: Earth and Environmental Science, 473(1), 012149.

Moreau, R. A., Whitaker, B. D., & Hicks, K. B. (2002). Phytosterols, phytostanols, and their conjugates in foods: structural diversity, quantitative analysis, and health-promoting uses. Progress in Lipid Research, 41(6), 457–500.

MS, U., Ferdosh, S., Haque Akanda, Md. J., Ghafoor, K., A.H., R., Ali, Md. E., … Islam Sarker, Md. Z. (2018). Techniques for the extraction of phytosterols and their benefits in human health: a review. Separation Science and Technology, 53(14), 2206–2223.

Murkovic, M., Piironen, V., Lampi, A. M., Kraushofer, T., & Sontag, G. (2004). Changes in chemical composition of pumpkin seeds during the roasting process for production of pumpkin seed oil (Part 1: non-volatile compounds). Food Chemistry, 84(3), 359–365.

Oka, Y., Kiriyama, S., & Yoshida, A. (1973). Sterol Composition of Fruits, Fungi, Marine Algae and Tea, Coffee and Cocoa. Eiyo To Shokuryo, 26(5), 317–327.

Orozco, J., Cortés, A., Cheng, G., Sattayasamitsathit, S., Gao, W., Feng, X., … Wang, J. (2013). Molecularly Imprinted Polymer-Based Catalytic Micromotors for Selective Protein Transport. Journal of the American Chemical Society, 135(14), 5336–5339.

Panda, S., Jafri, M., Kar, A., & Meheta, B. K. (2009). Thyroid inhibitory, antiperoxidative and hypoglycemic effects of stigmasterol isolated from Butea monosperma. Fitoterapia, 80(2), 123–126.

Piironen, V., Lindsay, D. G., Miettinen, T. A., Toivo, J., & Lampi, A.-M. (2000). Plant sterols: biosynthesis, biological function and their importance to human nutrition. Journal of the Science of Food and Agriculture, 80(7), 939–966.

Płotka-Wasylka, J., Marć, M., Szczepańska, N., & Namieśnik, J. (2017). New Polymeric Materials for Solid Phase Extraction, 47(5), 373–383.

Ramström, O., & Mosbach, K. (1999). Synthesis and catalysis by molecularly imprinted materials. Current Opinion in Chemical Biology, 3(6), 759–764.

Rosengren, A. M., Karlsson, B. C. G., & Nicholls, I. A. (2013). Consequences of Morphology on Molecularly Imprinted Polymer-Ligand Recognition. International Journal of Molecular Sciences, 14(1), 1207.

Rudkowska, I. (2010). Plant sterols and stanols for healthy ageing. Maturitas, 66(2), 158–162.

Salehi, B., Quispe, C., Sharifi-Rad, J., Cruz-Martins, N., Nigam, M., Mishra, A. P., … Koch, W. (2020). Phytosterols: From Preclinical Evidence to Potential Clinical Applications. Frontiers in Pharmacology, 11.

Schaller, H. (2003). The role of sterols in plant growth and development. Progress in Lipid Research, 42(3), 163–175.

Schuler, I., Milon, A., Nakatani, Y., Ourisson, G., Albrecht, A. M., Benveniste, P., & Hartman, M. A. (1991). Differential effects of plant sterols on water permeability and on acyl chain ordering of soybean phosphatidylcholine bilayers. Proceedings of the National Academy of Sciences, 88(16), 6926–6930.

Schwarz, L. J., Danylec, B., Harris, S. J., Boysen, R. I., & Hearn, M. T. W. (2016). Sequential molecularly imprinted solid-phase extraction methods for the analysis of resveratrol and other polyphenols. Journal of Chromatography A, 1438, 22–30.

Schwarz, L. J., Leung, B. K. Y., Danylec, B., Harris, S. J., Boysen, R. I., & Hearn, M. T. W. (2018). Phytosterol Recognition via Rationally Designed Molecularly Imprinted Polymers. C 2018, Vol. 4, Page 13, 4(1), 13.

Ścigalski, P., & Kosobucki, P. (2020). Recent Materials Developed for Dispersive Solid Phase Extraction. Molecules 2020, Vol. 25, Page 4869, 25(21), 4869.

Shen, X., & Ye, L. (2011). Interfacial molecular imprinting in nanoparticle-stabilized emulsions. Macromolecules, 44(14), 5631–5637.

Shiomi, T., Matsui, M., Mizukami, F., & Sakaguchi, K. (2005). A method for the molecular imprinting of hemoglobin on silica surfaces using silanes. Biomaterials, 26(27), 5564–5571.

Sinha, A., Basiruddin, S. K., Chakraborty, A., & Jana, N. R. (2015). B-cyclodextrin functionalized magnetic mesoporous silica colloid for cholesterol separation. ACS Applied Materials & Interfaces, 7(2), 1340–1347.

Soysal, M., Muti, M., Esen, C., Gençdağ, K., Aslan, A., Erdem, A., & Karagözler, A. E. (2013). A Novel and Selective Methylene Blue Imprinted Polymer Modified Carbon Paste Electrode. Electroanalysis, 25(5), 1278–1285.

Sundararaman, P., & Djerassi, C. (1977). A convenient synthesis of progesterone from stigmasterol. The Journal of Organic Chemistry, 42(22), 3633–3634.

Tang, Z., Liu, C., Wang, J., Li, H., Ji, Y., Wang, G., & Lu, C. (2016). Preparation and characterization of monodisperse molecularly imprinted polymers for the recognition and enrichment of oleanolic acid. Journal of Separation Science, 39(8), 1592–1602.

Vasapollo, G., Sole, R. del, Mergola, L., Lazzoi, M. R., Scardino, A., Scorrano, S., & Mele, G. (2011). Molecularly Imprinted Polymers: Present and Future Prospective. International Journal of Molecular Sciences 2011, Vol. 12, Pages 5908-5945, 12(9), 5908–5945.

Verleyen, T., Forcades, M., Verhe, R., Dewettinck, K., Huyghebaert, A., & de Greyt, W. (2002). Analysis of free and esterified sterols in vegetable oils. Journal of the American Oil Chemists' Society, 79(2), 117–122.

Wang, D., Hong, S. P., Yang, G., & Row, K. H. (2003). Caffeine Molecular Imprinted Microgel Spheres by Precipitation Polymerization. Korean Journal of Chemical Engineering 2003 20:6, 20(6), 1073–1076.

Wang, J., Huang, M., Yang, J., Ma, X., Zheng, S., Deng, S., … Zhao, P. (2017). Anti-diabetic activity of stigmasterol from soybean oil by targeting the GLUT4 glucose transporter. Food & Nutrition Research, 61(1).

Wulff, G. (1995). Molecular Imprinting in Cross-Linked Materials with the Aid of Molecular Templates— A Way towards Artificial Antibodies. Angewandte Chemie International Edition in English, 34(17), 1812–1832.

Yan, H., & Kyung, H. R. (2006). Characteristic and Synthetic Approach of Molecularly Imprinted Polymer. International Journal of Molecular Sciences 2006, Vol. 7, Pages 155-178, 7(5), 155–178.

Zhang, X., Yang, S., Jiang, R., Sun, L., Pang, S., & Luo, A. (2018). Fluorescent molecularly imprinted membranes as biosensor for the detection of target protein. Sensors and Actuators B: Chemical, 254, 1078–1086.